Numerical Modelling of Separation Efficiency of Sediments in a Combined Sewer Overflow (CSO)

Berit Bye Wilhelmsen

NTNU

Norwegian University of Science and Technology
Faculty of Engineering Science and Technology
Department of Hydraulic and Environmental Engineering

Date	Our reference
13-01-2012	R. Ugarelli

Memo

To:	Stud. Techn. Berit Bye Wilhelmsen
Copy to:	Paal Skjetne and Sveinung Sægrov
From:	Rita Ugarelli
Signature:	

Numerical Modelling of Separation Efficiency of Sediments in Combined Sewer Overflow (CSO)

Background

Climate changes will stress urban water systems resilience. In particular, the wastewater pipe infrastructure is expected to be the most in need of adaptation and even require the adoption of new solutions. New concepts should be developed for combined sewer overflows (CSOs) to adapt to expected conditions of climate changes. Both quantity (storage) and quality (treatment) performance in relation to climate change have to be addressed. The CSO should not only perform the function of protecting the system against overloads, but also serve as a point of rough wastewater pre-treatment to safeguard the quality of the receiving water bodies, which should be "good" both in terms of ecological status and chemical quality (Water Framework Directive 2000/60/EC).

Background of this Master thesis is the project work in "TVM4510 VA-teknikk FDE" (7.5 ECTS) at the Norwegian University of Science and Technology in autumn 2011. The project presents a study of literature on the impacts of climate change on combined sewer overflows (CSOs) combined with computational fluid dynamics (CFD). Based on knowledge on hydraulics in open channel flows and numerical modelling, flow phenomena in a transition were modelled successfully. The study was conducted as a preliminary work to prepare the author for a study on numerical modelling of sediment transport to be performed during the master thesis dealing with the tasks described below.

Project Tasks

1. The student will use an open channel model coupled to a discrete particle model (DPM) to study transport of sediments in channels. Once the model has been validated the possibilities in the particle tracking routine should be investigated.

Norwegian University of Science and Technology

2. A study of sediment transport will be undertaken for a CSO geometry from Århus municipality which is part of the FP-EU project PREPEARED. The effect of different flow fields on separation efficiency will be investigated for different particle types.

Assistance

Professor Rita Ugarelli, Department of Hydraulic and Environmental Engineering, NTNU will be the main contact for this work, assisted by Professor Sveinung Sægrov and by Paal Skjetne, PhD, SINTEF Material and Chemistry.

Presentation and Delivery

The project report shall be delivered in B5 format and front page received at the institute. The institute is economically responsible for two copies to the institute and one to the student. Extra copies shall be paid by the student.

Deadline: 9 July 2012

Preface and Acknowledgment

This is a Master of Science conducted at the Department of Hydraulic and Environmental Engineering at the Norwegian University of Science and Technology in spring 2012. It is a study of the quality performance of combined sewer overflows (CSOs) where separation efficiency of sediments is assessed with computational fluid dynamics (CFD).

I would like to thank my supervisor Professor II at NTNU Rita Maria Ugarelli for taking great interest in my work and progress and guidance in the writing process. Senior Researcher Paal Skjetne at SINTEF Material and Chemistry has been the main support with computer programming. Than you for sharing your expertise within the field of CFD and the inspiration you have given. The contributions of these two have been very important for this report, and I appreciate the guidance throughout the thesis.

I am thankful to SINTEF for economic support to attend an introduction course on FLUENT in Sheffield in September 2011. I also appreciate the technical support with the software FLUENT from Torbjørn Virdung, Jens-Uwe Frieman and Maciej Ginalski at ANSYS. I would thank Vegard Eide for guidance with submitting simulations on Notur High Performance computers. Access to this facility has reduced the computational time significantly and made it possible to run more simulations. Finally, I would also like to thank Wei Yang and Lars Hem at SINTEF and Sveinung Sægrov at NTNU for helpful response when consulted.

Trondheim, June 2012

Berit Bye Wilhelmsen

i

Abstract

Combined sewer overflows (CSOs) are a part of the combined storm water and foul sewer system. CSOs should protect the downstream sewer system against overloading during heavy rainfall and snow melting. This report investigates how three-dimensional computational fluid dynamics (CFD) can be applied to evaluate the quality performance of combined sewer overflows (CSOs).

Separation efficiency is a performance indicator defined as the fraction of sediments that are treated and not overflowing. Emissions from poorly constructed CSOs have a harmful impact on receiving water quality. Predicted increase in rainfall in the northern hemisphere due to climate change is enhancing stresses imposed on these structures.

EU established the Water Framework Directive (WFD) in 2000 to ensure good ecological and chemical quality for receiving streams and lakes. To meet this standard, a reduction in emissions of pollutants is required through improvement of separation efficiency of CSOs. Numerical modelling creates new opportunities for detailed analyzes of existing and new structures as such tools where not available when the first CSOs where built.

In this report, the assessment of a CSO with CFD is presented in the context of a geometry from Århus. The CSO is one of the case studies in the EU project PREPARED Enabling Change, which aims to adapt Europe's water supply and sanitation systems to climate change. It is a complex device with one inlet, four overflow chambers and two outlet pipes.

Prior to the modelling, a literature review was carried out to identify the characteristics of combined sewage. The purpose was to determine what particles that should be modelled and find appropriate boundary conditions.

The sewer quality showed large variations dependent on flow rate, locations inside the system and between different systems. The combined sewage consists of a mixture of organic and inorganic material and no unique relationship between density and particle size could therefore be found. A wide range of sediments with size $100\mu m$ - 5mm and densities $1002kg/m^3$, $1170kg/m^3$, $1400kg/m^3$, $1720kg/m^3$, $2000kg/m^3$ and $2650kg/m^3$ were therefore selected to represent sewer sediments in the numerical model.

At the bed of the CSO a criteria was needed to determine if a particle settled or was suspended in the fluid. A bed shear stress (BSS) boundary condition was found to be appropriate. The shear stress at the bed was compared to a critical value specified by the user. A study by Berg (1988) showed that the critical value for settling of particles in a combined sewer with sand traps was 1.0Pa.

The numerical modelling was done with the commercial software FLUENT. Analyzes where carried out for two scenarios; (1) filling of the CSO with throughflow to the treatment plant, and (2) during overflow to receiving waters. Three velocities was used (0.3m/s, 0.5m/s and 0.7 m/s) to test the influence of velocity on the separation efficiency.

The paper demonstrates how the discrete phase model (DPM) can be utilized to predict particle trajectories and final destination of particles and how this can be used to calculate separation efficiency. The conclusion is that the particle tracking routine was found to be suitable for analyzes of sediment transport and separation efficiency. Overall the CSO in Århus showed a good separation efficiency higher than

50% for all velocities. The exception was sand particles with size 100 μm and organic material with density $1170 kg/m^3$ and diameters up to 0.5mm. The results showed that velocity had a strong influence on separation efficiency and flow streamlines on the distribution of particles on the different overflows. It was crucial to define appropriate boundary conditions as it has a significant effect on the result. Difference in separation efficiency for different types of particles was most significant during slow flow conditions. A references to previous work has shown that the particle tracking routine probably overestimates the separation efficiency for high velocities (Stovin & Saul, 1998). In future work the results from Århus should be compared with measurements, to determine if this is the case for the Århus results as well.

CFD modelling in combination with modern measurement techniques provide great opportunities for optimization of CSOs. The intention is that this can serve as a pilot project for future research and work with adaption of CSOs under climate change.

Sammendrag

Dette er et studie av regnvannsoverløp i fellessystemet for overvann og spillvann. Regnvannsoverløp skal hindre overbelastning av nedstrøms anlegg ved kraftig regnvær og snøsmelting. Denne rapporten utforsker hvorvidt numeriske modeller kan bidra til å evaluere overløpenes forurensningskontroll.

Separasjonsgrad er en ytelsesindikator for forurensningskontroll og er definert som andelen sedimenter som ikke slippes ut i overløpsvannet. Utslipp fra dårlig konstruerte overløp har en skadelig virkning på resipienten. Forventet økning av nedbør på den nordlige halvkule på grunn av klimaendringer, øker belastningene på overløpene betraktelig.

I år 2000 innførte EU et nytt vanndirektiv for å sikre god økologisk og kjemisk kvalitet i resipientvassdragene. For å møte kravene i dette direktivet, må utslipp av forurensende stoffer reduseres gjennom forbedring av partikkelfjerning i overløpene. Numeriske modeller (CFD) skaper nye muligheter til å revidere kvaliteten av nye og gamle overløp med teknologi som ikke var tilgjengelig da de første overløpene ble bygget.

Dette er et eksempelstudie av bruken av CFD på et regnvannsoverløp i Århus. Overløpet er et av studieobjektene som er inkludert i EU prosjektet PREPARED Enabling Change som ønsker å tilpasse Europas vann- og avløpssystemer for å møte konsekvensene av klimaendringer. Overløpet har en komplisert geometri med et innløp, fire overløpsterskler og to utløpsrør til renseanlegget.

Før modelleringen, ble det gjennomført et litteraturstudie for å kartlegge egenskaper ved avløpsvann. Hensikten var å bestemme hvilke partikkeltyper som skulle modelleres og finne et passende kriterium for sedimentering.

Avløpsvannet viste stor variasjon i kvalitet avhengig av strømningsrate, mellom forskjellige ledningsnett og plassering innad i ledningsnettet. Ettersom avløpsvannet inneholder en blanding av organiske og uorganiske partikler, var det ikke mulig å finne en entydig sammenheng mellom partikkelstørrelse og diameter. Et bredt utvalg av sedimenter med diameter $100\mu m$ - 5mm and tetthet $1002kg/m^3$, $1170kg/m^3$, $1400kg/m^3$, $1720kg/m^3$, $2000kg/m^3$ og $2650kg/m^3$ ble derfor valgt ut for å representere typisk avløpsvann i modelleringen.

Langs bunnen av overløpet var det nødvendig å finne et kriterium for å avgjøre om en partikkel vil sedimentere eller forbli suspendert. Grensebetingelsen som ble valgt var et skjærspenningskriterie som sammenlignet skjærspenning langs bunnen med en kritisk verdi bestemt av brukeren. Den kritiske skjærspenningen ble satt til 1.0Pa som er den kritiske verdien for sedimentering av avløpsvann i fellessystem med sandfang i følge Berg (1988).

Den numeriske modelleringen ble utført i den kommersielle programvaren FLUENT. Analyser ble utført for to senarioer: 1) Oppfylling av overløpet med videreført vannmengde til renseanlegget, og 2) Ved utslipp fra overløpet til resipient. Betydningen av innløpshastighet for partikkelfjerningen ble testet.

Rapporten beskriver hvordan Discrete Phase Model (DPM) kan benyttes for å estimere partikkelbaner og finne hvor partiklene ender opp. Det blir demonstrert hvordan dette kan benyttes til å beregne overløpets separasjonsgrad. DPM modellen ble implementert med gode resultater og viste seg å være egnet for analyser av sedimenttransport og partikkelavskilling. Regnvannsoverløpet i Århus hadde høy partikkelf-

jerning med over 50% for alle hastigheter. Unntaket var små sandpartikler med diameter $100\mu m$ og organisk materiale med tetthet $1170kg/m^3$ og diameter opp til 0.5mm som gikk i overløp. Resultatene viste at innløpshastigheten hadde sterk innflytelse på partikkelavskillingen og strømningslinjene var bestemmende for hvor partiklene endte opp. Grensebetingelsene hadde også en stor påvirking på resultatene. Forskjellen i partikkelavskillingen mellom ulike partikkel typer var størst under rolige innstrømningsforhold. Tidligere studier har vist at DPM modellen trolig overestimerer partikkelavskillingsgraden for høye hastigheter (Stovin & Saul, 1998). Resultatene fra Århus modelleringen bør sammenlignes med målinger når dette foreligger.

Numerisk modellering kombinert med målinger har et stort potensial til å optimalisere overløp. Intensjonen er at denne rapporten skal være et pilotprosjekt for framtidig forskning og arbeid med tilpassning av regnvannsoverløp for klimaendringene.

Contents

List of Figures

List of Tables

List of Abbreviations

BOD .... biological oxygen demand
CFD .... computational fluid dynamics
CSO .... combined sewer overflow
DO .... dissolved oxygen
DPM .... discrete phase model
DRW .... discrete random walk
RWM .... random walk model
SS .... suspended solids
UDF .... user defined function
VOF .... volume of fluid
WFD .... water framework directive
WWTP .... waste water treatment plant

Chapter 1

Introduction

1.1 Combined Sewer Overflows (CSOs)

Combined sewer overflows (CSOs) function as flow regulators and a rough pre-treatment at outfall locations in the sewer network. During heavy rainfall or snow melting the flow is diverted in a through flow to the treatment plant and a spill flow to the receiving water bodies - streams, lakes and ocean, figure 1.1 (Huntington Sanitary Board, 2004). CSOs can also overflow due to clogging of pipes downstream in the sewer system.
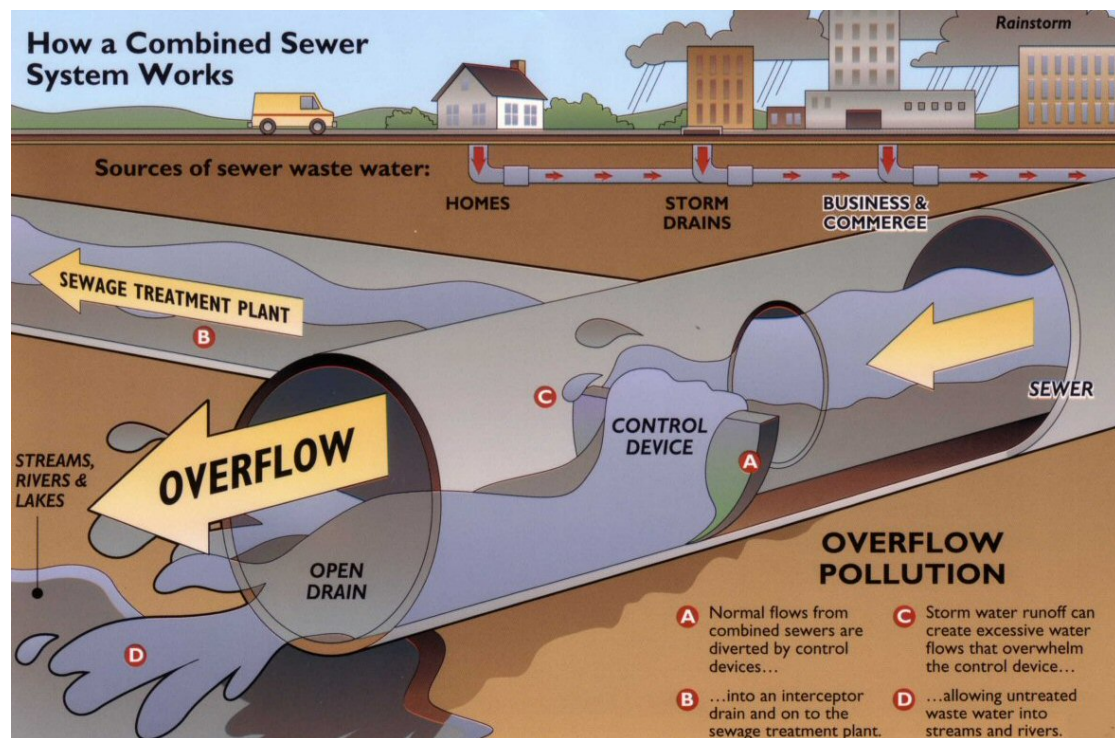
Figure 1.1: Principal drawing of combined sewer overflow (Huntington Sanitary Board, 2004).

1.2 Background

A project work by the author conducted during autumn 2011 addresses stresses imposed on CSOs due to climate change. In cold climate regions, one expects an increase in rainfall intensity and duration together with sea level rise and storm surge. The combined sewer systems do not have sufficient capacity, and climate change impacts are predicted to give a progressive increase in volumes discharged from CSOs. More frequent rainfall will give an increase in flushing of sediments because deposition state in the pipes is less often reached. Urbanization and deterioration of sewer systems are additional sources that enhance the stresses on CSOs.

Discharges from CSOs consists of a mixture of storm water, domestic, commercial and industrial waste water and sewer deposits. Concerns for receiving waters are oxygen reduction, eutrophication, toxic, aesthetic pollution, smell and health hazards. A special threat is imposed by heavy metals and persistent organic pollutants that are attached to the surface of particles from storm water runoff. Therefore the focus on CSOs today is to lessen the environmental pollution by improving the separation efficiency.

The Water Framework Directive (WFD) was established by EU in October 2000 to ensure good ecological and chemical quality in receiving water bodies (European Communities, 2000). To fulfil this requirement it is important with a holistic approach and system modelling can be used to reveal problem areas. Mitigating measures must be carried out in the catchment, the pipe network must be upgraded and maintained and separate systems should be built. These actions are however not enough and the performance of poorly constructed CSO devices must be strengthened. CSO emissions are a severe problem worldwide and there is a great need for rehabilitation. Upgrading and replacements of CSOs are comprehensive and costly work, but is inevitable to preserve the water bodies as required in the Water Framework Directive. New knowledge about the consequences of CSO pollution has given new requirements and design criteria.

1.3 Objective

The key objective of this study is to assess the performance of a CSO and identify its ability to retain sediments in the sewer system. Analysis should be undertaken to study how different sediments are affected by flow conditions. Three-dimensional numerical modelling should be used to investigate how this influences the solid separation efficiency. This paper aims to demonstrate the possibilities to model detailed hydraulics and sediment transport in complex geometries and give better understanding of the complex processes. Computational fluid dynamics (CFD) analyzing tools could contribute to the development of the next generation of combined sewer overflows.

As a starting point a simple open channel with a transition was used as a testing environment to get familiar with the discrete phase model (DPM). Then a complex CSO from Århus was modelled. The modelling approach and goals are presented briefly in table1.1.
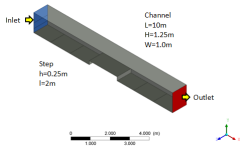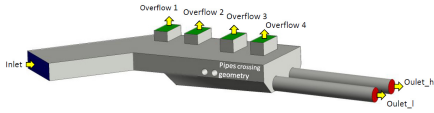
Modeling scenario	Modeling approach	Goal
Open channel 	VOF and DPM	Get familiar with modeling of sediment transport and validate the model.
Complex CSO in Århus 	Single phase model and DPM	Study separation efficiency for different types of sediments during a variety of flow conditions.

Table 1.1: Modeling scenarios.

1.4 Description of CFD Software - FLUENT

The fluid field in CFD is governed by the conservation equations of mass and momentum and is solved with the Reynolds average Navier-Stokes equations. The equations are discretized which means that they are transformed from integrals to algebraic equations. In CFD the domain is divided into grid cells. The algebraic equations are solved in all the grid cells with the finite difference method.

The commercial CFD software FLUENT from ANSYS was applied in this study. FLUENT offers state-of-the-art advanced capabilities to model laminar and turbulent flows as well as more complex physics including multiphase flows and particulate dynamics (ANSYS Inc., 2011a). An advantage of using a commercial code is that it has been extensively tested and verified. This study utilizes the volume of fluid (VOF) model to track a free surface of an open channel flow and the $k - \varepsilon$ model for turbulence. Particle tracks are predicted with the discrete phase model (DPM). Output can be obtained in all cells in the domain and can be presented as surfaces, pathlines, vector plots and contour plots. Particle tracks, residence time and particle fates at boundaries are output from the DPM model.

Chapter 2

Sediments in Combined Sewer

The purpose of this chapter is to study sewer sediment characteristics and processes for transport, erosion and deposition. This is the foundation of the modelling and is essential to choose the right methodology, define particle injections (particle density and size) and choose appropriate boundary conditions.

This chapter aims to answer the following questions. What is the quality of combined sewage? Which sediments present a threat to the environment and why? How can one obtain reliable measurements of the specific sewer system and why are there great variations over time and space? What mechanisms are used in movement of sediments? How can deposition of particles be related to shear stress? What would be an appropriate threshold value for bed shear stress to determine deposition in a combined sewer?

2.1   Waste Water Quality

Combined sewer systems carry domestic sewage, industrial waste water and storm water runoff. The sewer system carries both organic and inorganic material.

Organic compounds discharged to receiving waters can cause a reduction in dissolved oxygen (DO) as it is consumed in the decomposition process. In the Austrian regulations for CSO emissions ÖWAVRB 19 the criterion is that the oxygen level should be higher than 5mg/l (Kleidorfer & Rauch, 2011).

Clay, sand and gravel are inorganic material that mainly enters the sewer system with storm water. Pollutants are associated with these particles and it is important to understand the effect they have on receiving waters.

Nutrients and bacteria are attached to the surface of particles with diameter less than $50 \ \mu m$. Emissions of nutrients such as nitrogen and phosphorus can promote excessive growth of algae.

Heavy metals (Pb, Hg, Cd, Zn, Cu, Cr, Ni, W etc.) and organic micro pollutants (PAH, PCB, BETX, CHC, PFC) are also associated with inorganic particles. Sources for these contaminants are vehicles, building material, industry spills and de-icing (Paus, 2011), and they inflict a serious threat to the environment because they are toxic and persistent. A study conducted in the Bad Mergentheim sewer system in Germany documented that there was a relationship between the load of heavy metal and the settling velocities of particles (Michelbach & Wöhrle, 1992). 350 samples were analyzed for lead, cadmium, copper, nickel and zinc. As seen in figure 2.1, the particles with a settling velocity of 0.4 cm/s had the highest load of contaminants (Michelbach & Wöhrle, 1992).
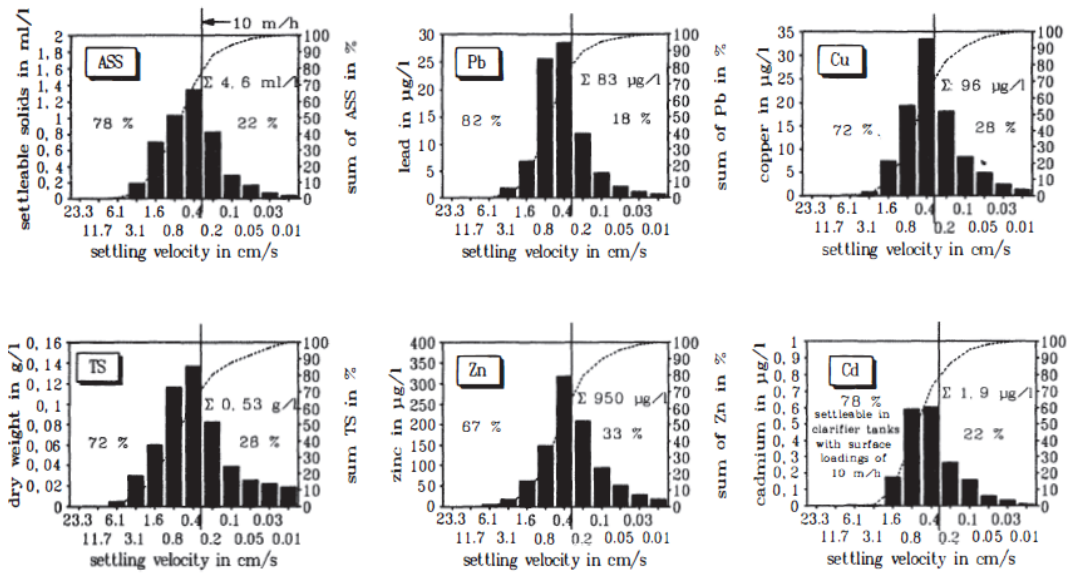
Figure 2.1: Relationship between settling velocity and heavy metals (Michelbach & Wöhrle, 1992).

2.1.1 Sampling Methods

Proper sampling and analysis must be done to assess the design and performance of CSOs. The locations inside the sewer and the time of sampling must be chosen carefully to get representative samples. Reliable measurements are important as they are used as input data in numerical modelling. The data should also be used for calibration and verification purposes. An investment in data collection can save extra costs by identifying problem areas and improving poorly constructed CSOs.

Sampling of sediments should be synchronized with flow measurements. Accurate flow measurements of velocities in three-dimensions can be done with an ultrasonic system and can be applied in large sewers (Ashley *et.al.*, 1993). Samples from the bed sediments can be done to find grain size distribution, densities and associated pollutants. Suspended solid samples should be taken from different locations in the flow field during variable flow conditions. Laser diffraction can provide information about particle sizes in the water column. Particle size distributions are measured from the angular scattering, figures 2.2 and 2.3. The bed level can also be monitored with a sonar system to get an indication of deposition and erosion (Ashley *et.al.*, 1993).
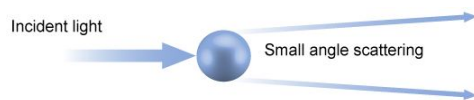
Figure 2.2: Laser diffraction - Angle scattering of a large particle (Malvern Instruments Ltd, 2012).
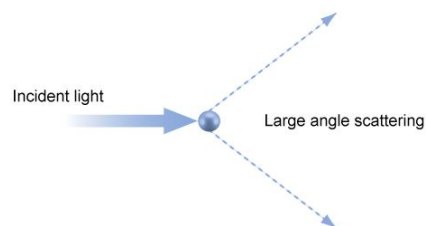
Figure 2.3: Laser diffraction - Angle scattering of small particle (Malvern Instruments Ltd, 2012).

5

2.1.2 Spatial Quality Variations

Every sewer system has its own waste water characteristics dependent upon its functions and area use in catchment. Accurate measurements of specific sewer systems are therefore vital to get information about the particle distribution and associated pollutants. Figure 2.4 illustrates the difference between different types of sewer systems and different locations (Berg, 1988). A storm water system, line 1, is compared to a combined sewer system, line 2. The storm water system has a higher particle mean diameter due to the content of gravel. The variations between different locations for combined sewer systems can be seen from line 1, which represents a sewer system in Gothenburg in Sweden, and in lines 3 and 4 from Trondheim in Norway.
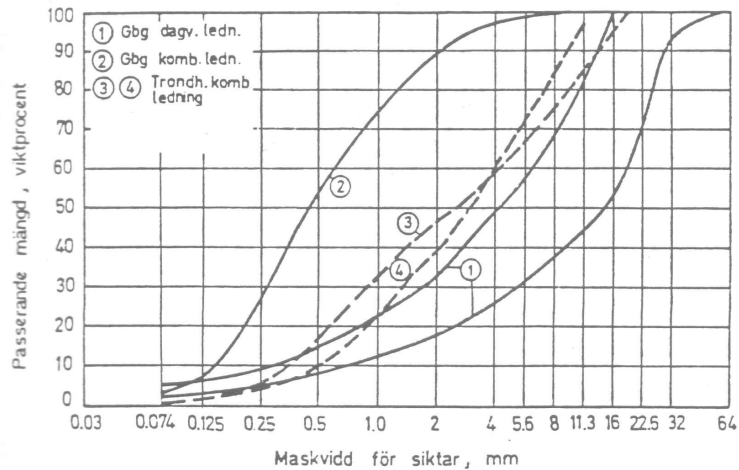
Figure 2.4: Grain size distribution for sediments in pipes. Lines 1 and 2 represents the Gothenburg sewer system in Sweden. Line 1 is the storm water system and line 2 is the combined sewer system. Lines 3 and 4 represent the combined system in Trondheim (Berg, 1998).

In addition to variations between sewer systems there can be local variations inside a specific sewer system. Figure 2.5 shows samples of sediments in different locations in a sewer system in Dundee, UK (Ashley & Crabtree, 1992).
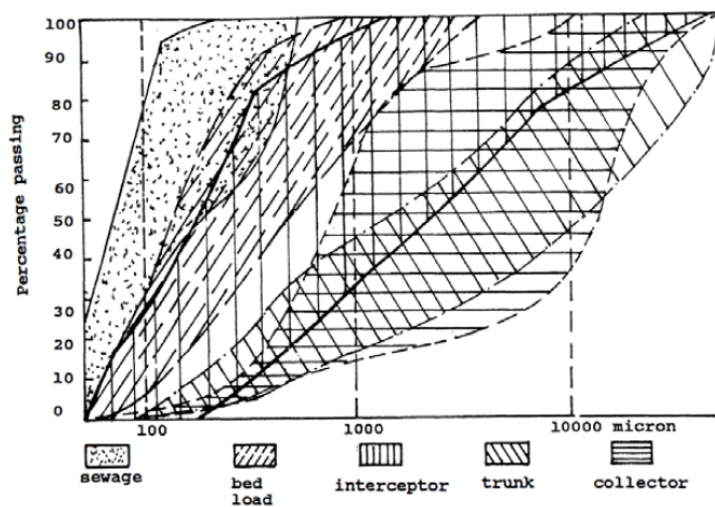
Figure 2.5: Local variations in sediment characteristics in Dundee sewer (Ashley & Crabtree, 1992).

6

PREPARED Enabling Change is a project commissioned by the European Union and is under the seventh framework program, FP7. The project started in February 2010 and is planned to end in January 2014. It has the purpose to adapt the water and sanitation systems to climate change. The results from this work will be demonstrated in 10 cities in Europe and the solutions should be exportable to other urban areas (PREPARED Enabling Change, 2012). INSA Lyon, Nivus and SINTEF have collaborated on work area 3, which has the purpose to improve the use of sensors and models. In conjunction with this work, the location of water quality sensors where considered. The following aspects must be considered according to PREPARED report no. 2011.031 (2011):

- Flow conditions change locally in the sewer system, i.e. at overflows, bends, junctions and pumps, and can produce errors;

- Practical considerations such as accessibility, safety of staff, equipment, connection to electric and communication networks must be taken;

- The location of sensors should be in areas where particles do not concentrate or alternatively in areas with old deposits;

- The average amount of particles is approximately half the value of concentration measured at the bottom, figure 2.6; and,

- Sensor should not be located in the center of the pipe, but a little bit over the bed as illustrated in figure 2.7. The measurements must then be multiplied with the percent of concentration that are lost due to lifting of the sensor up from the bottom.
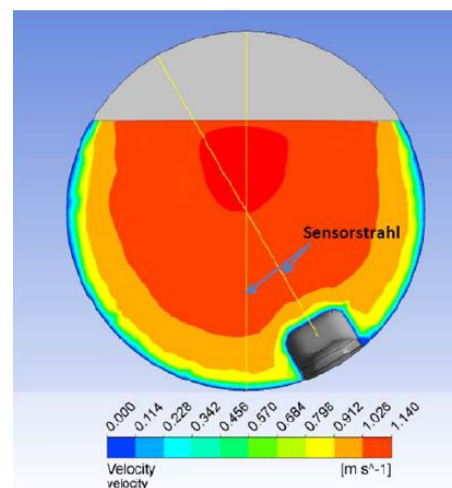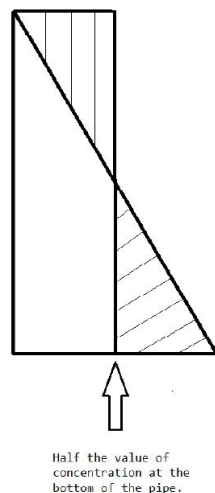
Figure 2.6: Correlation between depth and concen-Figure 2.7: Sensor location in a pipe (Vosswinkel, tration of sediments (Bruaset *et al.*, 2011). 2010).

2.1.3 Time Induced Quality Variations

Weather conditions induce time variations of storm water. A well known phenomena is the $first\ flush$ were high concentrations are discharged during a short period. Ashley $et\ al.$ (1992) summarized the main factors influencing the first flush as:

- Contributing impermeable catchment area;

- Rainfall intensity;

- Antecedent dry period;

- Cleanliness of sewer network;

- Location and type of sewer network; and,

- Sewer gradients and local hydraulics.

Seasons are also important, especially in cold climate regions, where contaminants concentrated in snow can result in significant pollution when snow melts. High flow rates will carry larger particles than dry weather flow. This will affect the mean particle diameter, d_{50}, as illustrated in figure 2.8, a graph for storm water. Small particles are mostly affected by an increased discharge.
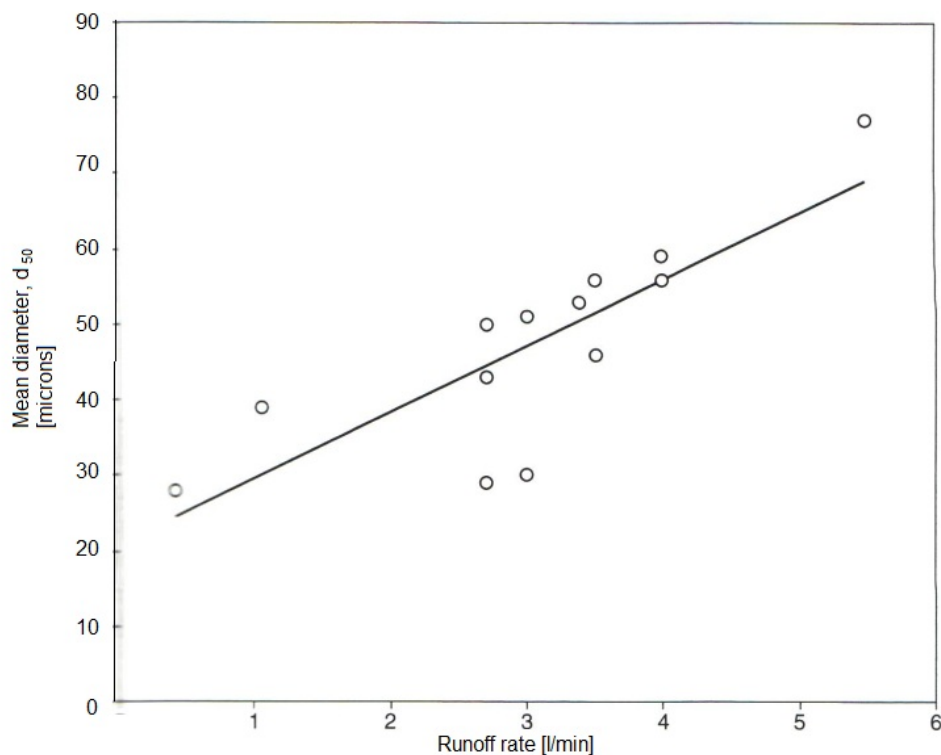
Figure 2.8: Relationship between median particle size and flow rate (Butler & Davis, 2011).

The water level in the sewer system has variations in time dependent on stormwater runoff and pumping in the system.

2.1.4 Sediment Characteristics

Sediments can be characterized by density, particle diameter and shape and settling velocity. Figure 2.9 illustrates sediment size, through a grain distribution curve, based on particle diameter and a volume fraction. Particles that can be found in sewers range in size from less than $100\mu m$ to10mm.
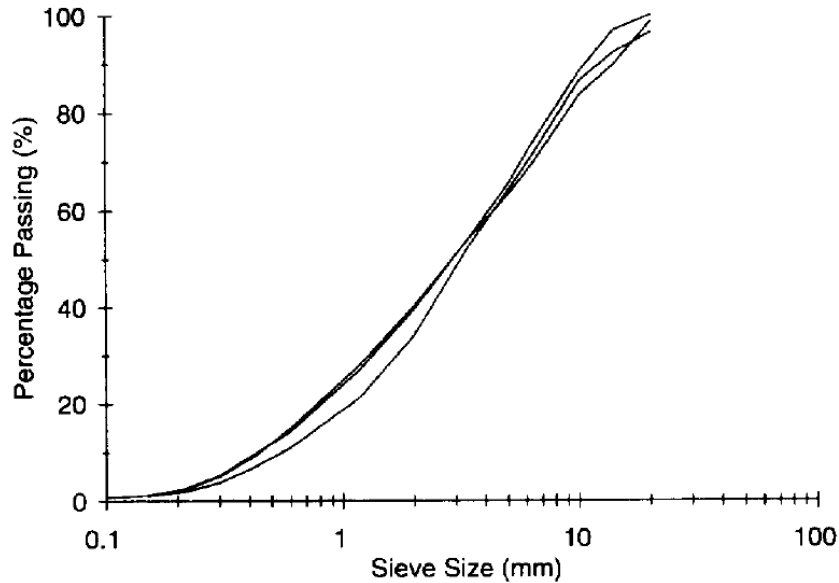
Figure 2.9: Grain size distribution of deposits from Dundee sewer (Bruaset *et al.*, 2011)

A review on relevant literature has shown that there is considerable data available on grain size distributions. However, this information is not connected to particle densities. At SINTEF senior research scientist Lars Hem and research manager Herman Helness were consulted on the relationship between particle sizes and densities in combined sewers. They could not provide any specific data on this, as the research on the matter is limited in both raw water, activated sludge and treated water. According to Herman Helness, the density of the organic material should be slightly higher than water (Helness, personal communication, March 14, 2012)

All grain sizes of inorganic material have a density of $2650 kg/m^3$. For inorganic material, however, it is impossible to choose one typical density since the variations are so significant. Some studies are included in the following to illustrate this and to provide a background for the modelling approach:

- Butler and Davies (2000) presented a coarse categorization with a particle sizes and corresponding density range, shown here in table 2.1.

Sediment type	Particle diameter, d	Density $[kg/m^3]$
Gross solids	> 6 mm	900 - 1200
Grit	1.5 mm - 6 mm	2650
Suspended Solids	0.45 μm - 1.5 mm	1400 -2000

Table 2.1: Coarse categorization of solids in sewer systems (Butler & Davis, 2000).

- Saul and Svejkovsky (1994) divided between floatables with density $998 kg/m^3$ and sinkers with density 1002 kg/m^3 and modelled particle sizes 2 mm and 6 mm for both types;

- Field and O'Connor (1996) used grit with density $2650 kg/m^3$ and heavy organics with density $1200 kg/m^3$. Heavy organics were in the range 0.2mm < d < 5mm;

9

- Pollert and Stransky (2002) studied the particles with 0.0001mm < d < 1mm due to their danger to the environment. Densities were in the range 1300 kg/m^3, $1500kg/m^3$, $1800kg/m^3$ and $2600kg/m^3$; and,

- Ashley and Crabtree (1992) divided bed load in a bottom layer with density $1720kg/m^3$ and a top layer with density $1170kg/m^3$.

2.2 Movement of Particles

Particles are transported in fluid, settling or re-suspending. Erosion and sedimentation is constant and dynamic processes, dependent on hydraulic conditions and sediment characteristics. The nature of sewer sediments is complex and heterogeneous, and the physical processes are not yet fully understood. The age of the sediments can for example influence how consolidated the deposits are. Old deposits would have higher resistance against erosion due to the cohesion in organic material. A concern with climate change is that the state of stable deposits will be reached less often. An increased frequency of rainfall will therefore result in more erosion of sediments.

2.2.1 Sediment Transport

Sediment transport has traditionally been categorized as bed load and suspended load. In between these two we have saltation that is a leaping movement of the sediments. There is no clear boundary between the different transport modes as this change with flow conditions. Raudkivi (1998) has indicated some loose boundaries between the different modes dependent on the shear velocity, $U_* = \sqrt{\frac{\tau_0}{\rho}}$, and settling velocity, W_s, of the particles. When $\frac{W_s}{U_*} > 0.6$ the transport mode is in suspension, while $0.6 < \frac{W_s}{U_*} < 2.0$ is saltation and $2.0 < \frac{W_s}{U_*} < 6.0$ is bed load.

2.2.1.1 Suspended Load

Suspended load is defined as particles that are carried along in the fluid for some time. During dry weather flow there is a gradient in the suspended sediment concentration as illustrated in figure 2.10 (Ashley et al., 1992). When the flow conditions changes during a storm event, the concentration of suspended sediments are increased and the sediments are mixed. Suspended solid concentration is dependent on what happens upstream in the pipe at an earlier time, and does not react immediately to a change in flow conditions.
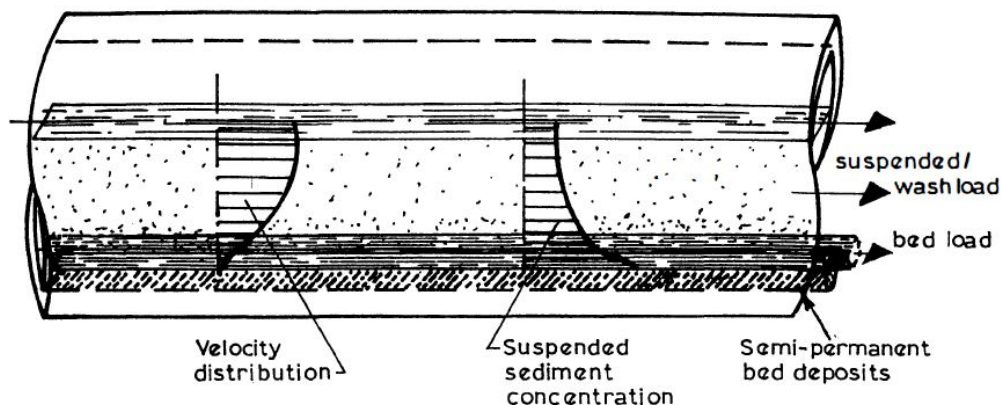
Figure 2.10: Velocity profile and suspended sediment concentration during dry weather flow (Ashley *et al.*,1992).

2.2.1.2 Bed Load

In rivers, bed load is defined as material rolling and sliding along the bed. However, in sewer systems the transport is more complex due to the heterogeneous character of the sediments and mixture of organic and inorganic material. The bed load can be considered as a continual flow with a "dense cloud" of particles that moves along the bottom or on top of permanent deposited sediments. Numerical modelling of this phenomena has been done by using the volume of fluid (VOF) model and defining the bed load as a density current with a higher density than water (Schmitt *et al.*, 1999).

Ashley and Crabtree (1992) studied bed load and divided it into two main types, A and C; figure 2.11 (Butler & Davis, 2000). It should be noted that these densities represent a mixture of organic and inorganic material. Type A, at the bottom consists of coarse and loose granular material with a density around $1720kg/m^3$. On top of this layer there is a layer of fine-grained sediments with an average density of $1170kg/m^3$. This material is also deposited in sags in the system.

Type D
Type C
Type A,B
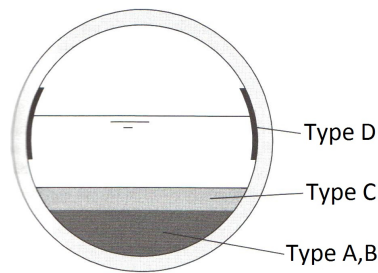
Figure 2.11: Cross section of sewage in a pipe (Butler & Davis, 2011).

The transport capacity and the quality of the sewer system have a strong correlation. The quality of the sewer system can be quantified by the relative sag volume (Berg, 1988). Sediment accumulates in dry weather periods and is washed out in the first flush. Type C sediments consist of mainly organic material, are easily erodible and will be re-suspended in the flow with an increasing discharge, as in figure 4.7. A study of CSO discharge that compared a storm water system with a combined sewer system showed that in a first flush event, 90% of the total biological oxygen demand (BOD) concentration originates from deposits in the sewer system (Hogland et al., 1992).

Bed load TYPE C sediment

TYPE A Sediment
Dry weather flow

Bed load TYPE A sediment
Onset of storm

POLLUTANT FRACTIONS
Associated with sediment
Readily erodible
Dissolved / fine
Readily settleable
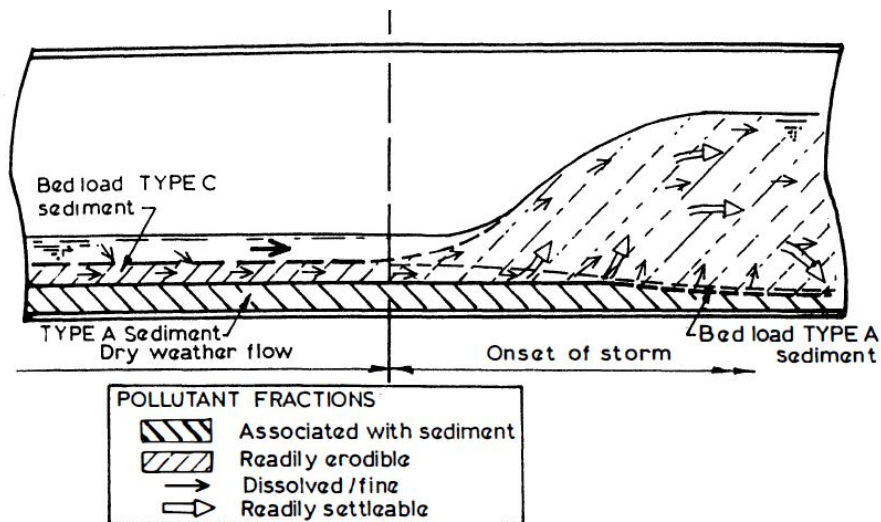
Figure 2.12: Erosion of bed load during wet weather flow (Ashley *et al.*, 1992).

Sediment type A presents the most severe threat to the environment due to the pollutants associated with inorganic material, section 2.1.

2.2.2 Sedimentation Mechanisms

The settling characteristics of suspended solids (SS) is important for the efficiency of a CSO. Surface load, v_o, is an important parameter in the design of sedimentation basins. It is the ratio of inflow, Q, and the horizontal area of the chamber, A; equation 2.1. Ideal conditions with laminar flow are assumed.

$$v_o = \frac{Q}{A} \tag{2.1}$$

If the settling velocity of the particles, v_s, is higher than the surface load, they will deposit according to Hazens' theory, equation 2.2 (Luyckx, Vaes & Berlamont, 2005). This is illustrated in figure 2.13.

$$Ha = \frac{v_s}{v_o} \tag{2.2}$$
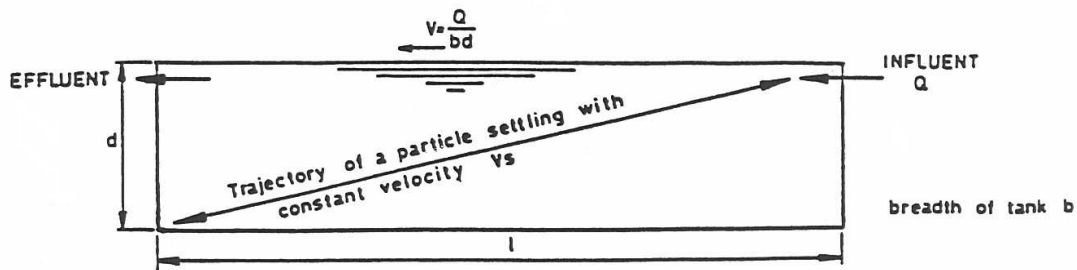
Figure 2.13: Principal drawing of sedimentation of a suspended particle according to Hazen (Luyckx, Vaes & Berlamont, 2005).

The settling velocity, v_s, of a particle can be found from Stokes' law, equation 2.3. Stokes' law is valid for small particles with particle Reynolds' number, equation 2.4, less than 0.3 (Nazaroff & Alvarez-Cohen, 2001). For water, this means particles with diameter less than $\backsim 100 \mu m$. Settling velocities of larger particles can be found by Hazens' tables.

Stokes' law:
$$v_s = \frac{C_c g d_p^2}{18} (\frac{\rho - \rho_f}{\mu}) \tag{2.3}$$

where C_c is a correction factor that is one in water, ρ is the density of the particle, ρ_f is the density of the fluid and g is the gravitational force.

Particle Reynolds' number:
$$Re_p = \frac{d_p V_\infty}{\nu} \tag{2.4}$$

where d_p is the particle diameter, V_∞ is the speed of the particle relative to the fluid and ν is the kinematic viscosity of the fluid.

The flow pattern in a CSO is not laminar, so turbulence will influence the sedimentation and erosion processes. Residence time can be used to find still zones where particles will deposit. This can be found by tests with tracers, or can be modelled numerically with particle tracking.

2.2.3 Critical Bed Shear Stress for Settling of Particles

Traditionally, bed shear stress is a parameter used to determine erosion. To ensure self-cleansing in pipes the bed shear stress should be higher than 3-4 N/m^2 (Pipelife Norge AS, 2000). A study by Stotz and Krauth (1986) suggested that it took less than 12 hours for the bed to develop significant strength. The discharge that gives the required shear stress should therefore be obtained in a 24-hour period and last in 10% of this time. Erosion in pipes is also of importance in a study of CSO performance as most of the sediments discharged from CSOs originate from deposits. Bed shear stress can be calculated using equation 2.5 where ρ is the density of the fluid, g is the gravitational constant, R is the hydraulic radius and S_0 is the energy slope.

$$\tau_0 = \rho g R S_0 \tag{2.5}$$

Bed shear stress can also be used in relation to deposition. A user defined function (UDF) for the bed boundary condition can be made, appendix 1. The UDF should compare the local shear stress with a critical value set by the user. If the shear stress is higher than the threshold value, the particle will be transported with the fluid, otherwise it will deposit. How this boundary condition is applied in a numerical model is described in more detail in section 4.2.5.2.

This section aims to find a threshold value for the bed shear stress that would be representative for typical combined sewer sediments. The critical shear stress value is dependent on the sewer characteristics and composition. The shear stress that is required to erode deposited material is higher than the shear stress that would make a particle deposit. With the assumption of uniform particles, Shields' diagram (figure 2.14) can be applied to find the relation between particle size and critical shear stress. Shields diagram is based on laboratory experiments and is valid for uniform material with density $2650 kg/m^3$ (Berg, 1988).
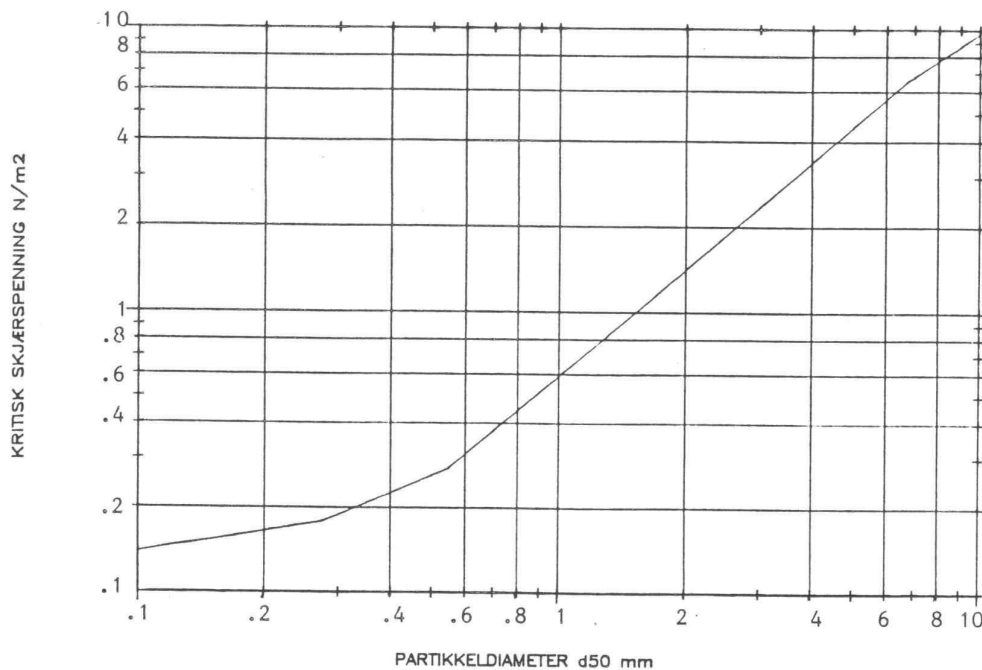
Figure 2.14: Critical shear stress as a function of diameter from Shield (Berg, 1988).

In conjunction with a project on self-cleansing in sewer pipes, Shields' criterion was adapted to different sewer types (Berg, 1988). Table 2.2 shows the recommended critical shear stress values that should be used to avoid deposition in sags in the sewer system. The corresponding mean diameter, d_{50}, could be found from Shields diagram, figure 2.14 (Berg, 1988). Based on this study a threshold value for the shear stress of 1,0 N/m^2 was chosen to represent a combined sewer system with sand traps.

Sewer type	Required local shear $[N/mm^2]$	Mean diameter [mm]
Separate sewer	0,5	0,9
Combined sewer with sand traps	1,0	1,6
Combined sewer and storm draining with high sand transport	1,5	2,1

Table 2.2: Recommended critical shear stress for different sewers.

Chapter 3

CSO Performance

In Norway, only 10% of the CSOs are built with the best available technology (Aaby, 2011). This is not only the situation in Norway, but is a problem world wide. In the United States 772 communities have problems with CSOs. Portland in Maine has in resent years invested $94 million in fixing CSOs and have planned to use $170 million the next 15 years (Wickenheiser, 2012 May 4).

This chapter aims to give the requirements for the status that should be obtain in receiving waters and present some performance indicators of the quality function of CSOs.

3.1 The Water Framework Directive

The Water Framework Directive (WFD) was established by EU in October 2000 as a holistic system for water management with the aim to protect the aquatic ecology, unique habitats, drinking water resources and bathing water. This means that the water quality should reflect a good ecological and chemical quality. According to the framework good ecological status allows a slight departure from the biological community which would be expected in conditions of minimal anthropogenic impact. Good chemical status is defined in terms of compliance with all the quality standards established for chemical substances at European level (European Communities, 2000). The classification process is illustrated in figure 3.1 (Toffol, 2006).

Figure 3.1: Classification process of the surface water based on CIS-VG2.3 (Toffol, 2006).

3.2 Legislation for CSO Emissions

De Toffel (2009) performed a comparativ study of regulations for urban drainage systems in different countries. The work concluded that there are not one unique defined performance indicator for CSOs, but variations between countries. Different performance indicators for 16 countries in Europe and The United States are presented in appendix 2. CSO emission criteria could be based on overflow frequency per year, mean annual overflow volume or maximum overflow discharge. In Austria, a standard ÖWAV-RB (2007) gives the requirements for particle separation dependent on the capacity of the WWTP and rainfall intensity, table 3.1 (Kleindorfer & Rauch, 2011). The rainfall intensity has a duration of 12 hours and a return period of 1 year (r720,1). Interpolation should be used for values not mentioned.

	Dissolved pollutants, η_d		Particulate pollutants, η_{CSO}	
Rainfall intensity /WWTP capacity	PE$\leq$ 5000	PE$\geq$ 50000	PE$\leq$ 5000	PE$\geq$ 50000
$r720, 1 \leq 30mm/12h$	50%	60%	65%	75%
$r720, 1 \leq 50mm/12h$	40%	50%	55%	65%

Table 3.1: Austrian requirements ÖWAV-RB 2007 for CSO efficiency (Kleindorfer & Rauch, 2011).

3.3 CSO Performance Indicators

Performance indicators can be used to measure the efficiency of a CSO over a long period, e.g. a 10 year period, or during a specific storm event. Numerical modelling also presents the possibility to model separation efficiency for different flow conditions. This section gives a presentation of performance indicators used to assess the quality aspect of a CSO concerning particle separation.

The flow split can be defined as the fraction of water that is not overflowing, equation 3.1. Here V_R is the storm water inflow volume and V_O is the volume overflowing and entering the receiving waters. The foul sewage is considered as constant while storm water runoff varies.

$$Flow\ Split = \frac{Volume\ Retained\ in\ System}{Volume\ Inflow} = \frac{V_R - V_O}{V_R} \qquad (3.1)$$

The flow split will have an influence on how much of the dissolved particles are discharged into receiving waters. If one assumes that it is a perfect mixture of wastewater, η_d, can be found from equation 3.2. Here C_C is the concentration of sediments in the inflow and C_O is the concentration overflowing to the receiving waters.

$$Separation\ of\ Dissolved\ Particles \Rightarrow \eta_d = \frac{V_R \cdot C_c - V_O \cdot C_O}{V_R \cdot C_c} \qquad (3.2)$$

Kleindorfer and Rauch (2011) defined the separation efficiency of a CSO as the fraction of surface water that should be treated, equation 3.3. In other words the particles that are settled in the CSO chamber and later removed and the sediments that continue to the WWTP.

$$Separation\ Efficiency\ of\ Settable\ Solids = \frac{Particle\ Load\ Retained}{Particle\ Load\ Inflow} \Rightarrow \eta_p = \frac{C_c - C_O}{C_c} \qquad (3.3)$$

In a numerical model, the separation efficiency can be calculated with the same method. The notation is different as it is based on the particle fates when a particle trajectory terminates at a boundary; equation 3.4. The particle fate is the status for the particle at the boundary, e.g. trap or escape. Here N_{tot} is the total number of particles injected in the inflow and N_{escape} are the particles overflowing.

$$\eta_{CSO,modelled} = 1 - \frac{N_{escape}}{N_{tot}} \qquad (3.4)$$

In addition to separation efficiency one can study the retention efficiency. Faram and Harwood (2003) defined this as the ability to retain previously separated sediments. This could be studied by injecting particles directly into the sediment storage regions. The results from such a study showed that the retention efficiency was consequently higher than the separation efficiency figure 3.2. The retention efficiency was significantly higher for the largest particles.
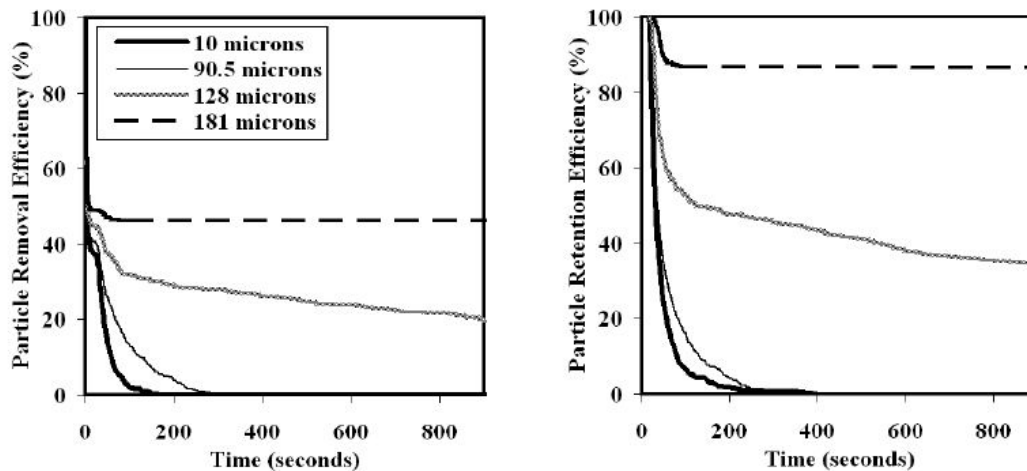
Figure 3.2: Separation efficiency (here: removal efficiency) and retention efficiency (Faram & Harwood, 2003).

3.4 Factors Influencing the Performance of a CSO

The efficiency of a CSO depends on the following conditions (Berg, 1988):

1. Surface load which is a function of width and length of the tank and the flow rate. The detention period will determine if small particles settle.

2. The velocity of the fluid and the corresponding shear stress decides if a particle at the bed will settle out or be transported as bed load.

3. The volume of the tank and the ratio of fullness will decide the capacity of the tank and affect 1. and 2.

The separation efficiency of settable particles can be improved by optimizing the CSO design, while the amount of dissolved particles only can be reduced by reducing the volume discharged from CSOs.

Separation efficiency depends on the flow rate and could therefore be presented as a function of the inlet velocity; figure 3.3 (Stovin & Saul, 1996). The removal of sewer solids is also dependent on the sediment characteristics and can be plotted as a function of settling velocity of Hazens' number; figure 3.4 (Luyckx, Vaes & Berlamont, 2005).
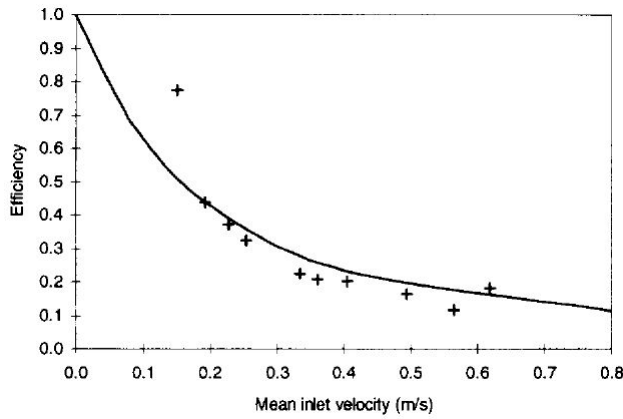
Figure 3.3: Separation efficiency as a function of velocity (Stovin & Saul, 1996).
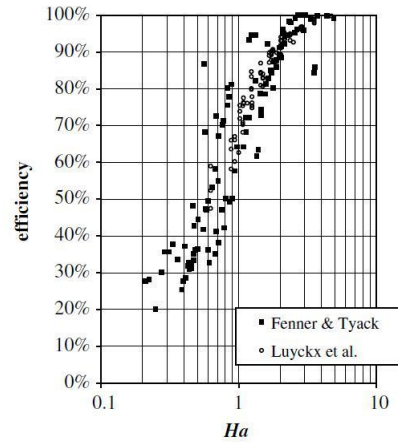
Figure 3.4: Separation efficiency as a function of Hazen number (Luyckx, Vaes & Berlamont, 2005).

Separation efficiency can also be presented as a function of the Froude number at the inlet, figure 3.5 (Luyckx *et al.*, 1999).
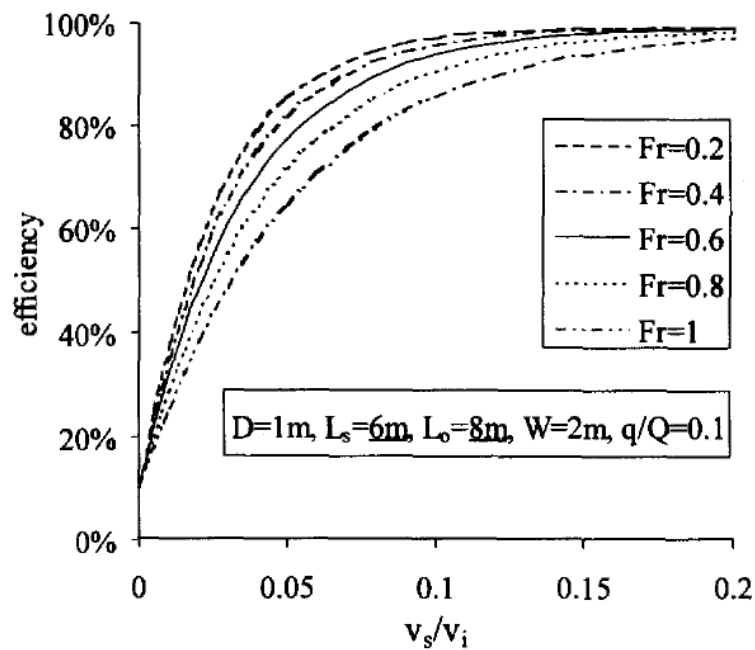
Figure 3.5: Separation efficiency as a function of Froude number at inlet (Luyckx *et al.*, 1999).

Chapter 4

Numerical Modelling

The purpose of this chapter is to introduce the numerical modelling concepts of sediment transport. First, turbulence modelling is discussed briefly as it has an effect on sediment trajectories. The focus is on the discrete phase model (DPM); particle injections, coupling between the particles and the continuous phase and boundary conditions. Sensitivity of separation efficiency for different input parameters is also discussed.

4.1 Turbulence Model

A turbulent flow is characterized by eddies fluctuating in time and scale. The most widely used turbulent model is k-ε and has the advantage of being robust and gives reasonable accurate results. More about turbulence modelling can be found from literature (ANSYS Inc., 2010b).

4.1.1 Turbulence near Wall.

When the turbulent flow approaches the wall, eddies are reducing in size. The flow goes from fully turbulent through a transition zone and becomes laminar close to the wall, figure 4.1 (ANSYS Inc., 2011a). In this process energy is transferred from eddies into viscous forces. To capture the transition from turbulent to laminar flow, a near wall turbulence model must be used. The size of the cells near the boundary is also of great importance and can be measured by the y+ value.
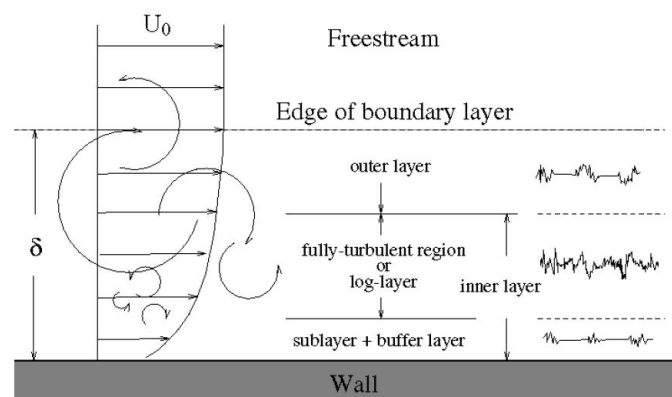
Figure 4.1: Turbulence near wall (ANSYS Inc., 2011a).

4.2 The Discrete Phase Model (DPM)

4.2.1 Limitations of the Model

It is important to recognize the presumptions a model is built on and be aware of the limitations. The DPM model does not include interactions between particles. The particles are not able to "see each other", and the concentration of particles in a cell can thus be greater than one. Consequently particle collisions and accumulation of sediments can not be accounted for. Since the DPM model neglects the volume of particles it is only valid when the volume fraction of particles is less than 10-12%. This must be the situation at the inlet regions but also inside the domain in regions with accumulation.

Sewage can be considered as a dilute mixture and the DPM model is therefore a suitable approach. Even though the model is not capable of simulating a build up of sediment layer, it is capable of monitoring in what regions there will be accumulation.

4.2.2 Particle Tracking

The DPM model calculates particle trajectories by integration of the particle force balance showed for the x-direction in equation 4.1 (ANSYS Inc., 2010b).

$$\frac{du_p}{dt} = F_D(u - u_p) + \frac{g_x(\rho_p - \rho)}{\rho_p} + F_x \tag{4.1}$$

Where u_p and ρ_p are the velocity and density of the particle and u and ρ are the properties of the fluid. F_D is the drag force and is a function of the relative velocity between the continuous phase and the particle. The second term, $\frac{g_x(\rho_p - \rho)}{\rho_p}$, represents the gravity force and does only apply in the y-direction. Additional forces specified by the user can be included in F_x.

Stovin and Saul (1998) studied the efficiency of a storage chamber to concentrate sediments. In conjunction with this work they performed a sensitivity analysis on the particle tracking parameters in the DPM model. The particle tracking parameters that must be specified is the number of time steps and the step length factor for the calculation of particle trajectories. Stovin and Saul concluded that the default value of 5000 for the number of time steps was too low as seen in figure 4.2. It is important to set this value high enough so, particle tracks are not aborted before the particles reach the outlet. The value should reflect the size of the domain, but 50 000 could be used as a starting point. The step length factor on the other hand was found to have minimal impact on the results as seen from the graph on the right side in figure 4.3 (Stovin & Saul, 1998).
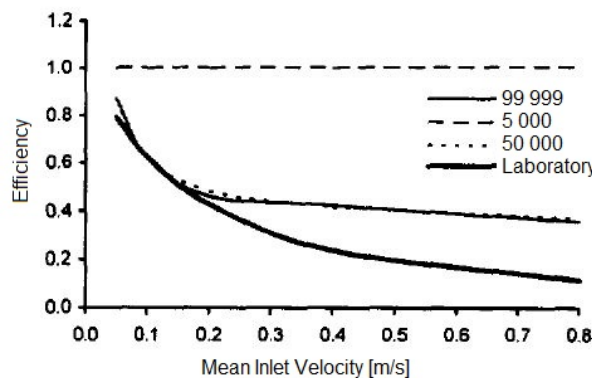
Figure 4.2: Sensitivity analysis of number of time steps (Stovin & Saul, 1998).
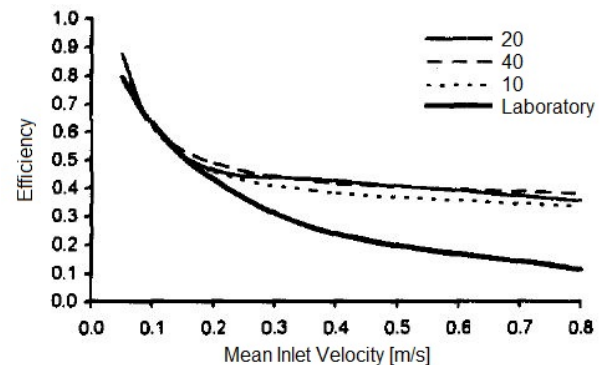
Figure 4.3: Sensitivity analysis of step length factor (Stovin & Saul, 1998).

4.2.2.1 Turbulent Dispersion

Turbulent dispersion calculates random fluctuations in the fluid and predicts more options for particle trajectories. Turbulent dispersion can be included with stochastic tracking with the discrete random walk model (DRW). Instead of using the mean velocity, $\overline{u}$, in the trajectory calculations, velocity fluctuations are introduced, u', $u = \overline{u} + u'$. Equation 4.2 shows how the local variation in velocity was calculated.

$$u^{'} = \zeta \sqrt{\overline{u'^2}} \tag{4.2}$$

Here ζ is a normally distributed random number and $\sqrt{\overline{u'^2}}$ is an expression for the kinetic turbulence.
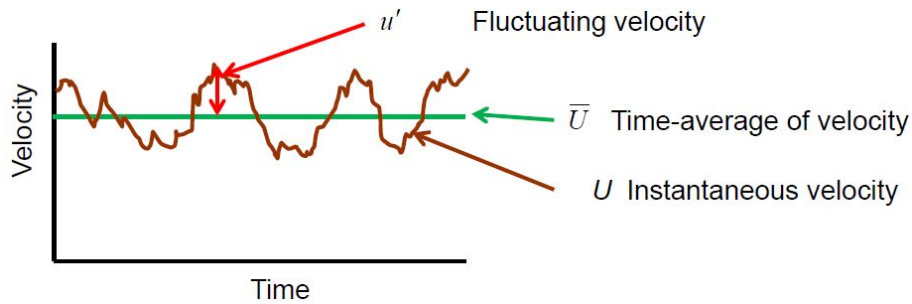
Figure 4.4: Fluctuating velocities.

According to Stovin and Saul (1998) several simulations must be run to obtain consistent results with the stochastic tracking. They found that 50 simulations gave a maximum deviation of $\pm 2.5\%$ from the population mean with a 99% confidence interval.

4.2.3 Coupling with Continuous Phase

Particle trajectories can be predicted with an uncoupled, or coupled solution strategy.

When the mass loading is low, the discrete phase does not interact with the continuous flow field and an uncoupled approach ("one-way coupling") can be applied. The particle trajectories are based on a fixed continuous flow field, figure 4.5, where drag forces and turbulence influences particles.

When particles are exchanging information as the mass and momentum with the continuous phase it is a coupled approach ("two-way coupling") , figure 4.6. Coupling between the particles and continuous field should be applied when the volume fraction of particles is higher than 2-3%.
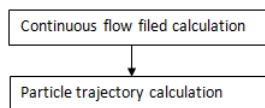
Figure 4.5: Uncoupled calculation process (ANSYS Inc., 2010b).
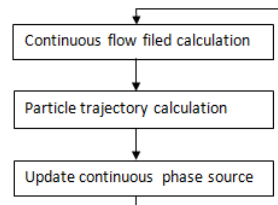
Figure 4.6: Coupled calculation process (ANSYS Inc., 2010b).

4.2.4 Particle Injections

Particles can be injected from as single, group, cone, file or surface. When particles are injected from a surface, as the inlet, the total number of particles, $N_{p,tot}$, that is injected is given in equation 4.3. If turbulent dispersion is included this must be multiplied with the number of stochastic tries. Harwood (1998) found that at least 500 particle injections were required to produce statistically valid efficiency predictions.

$$N_{p,tot} = N_{surface,cells} N_{parcels} \qquad (4.3)$$

The user must specify the total mass flow that is injected per unit time [kg/s] and this is distributed in different parcels. Parcels contain particles of the same type and are packages with the same properties (size and density). It is not possible to simulate all particles individually because of the high computational effort required.

There are two different approaches to how particles can be injected:

- Several uniform injections which mean one injection for each particle type. ; or,

- One injection based on a Rosin-Rammler distribution. Statistical properties as the mean, min and max diameters are input data.

The Rosin-Rammler distribution only allows a distribution of grain sizes and not densities. As organic material contains different densities, this is regarded as an important aspect of the study of a CSO. Several uniform injections gives good control of the particles injected.

The accuracy of particle trajectories is dependent on how particle injections are defined. Stovin and Saul (1998) analyzed how the particle size and injection type would influence the separation efficiency in a storage tank. 100 particles where injected in a horizontal line or vertical line and tested for three particle sizes according to table 4.1. The results presented in figure 4.7 shows that the efficiency is very sensitive to injection location, and particle size has less influence.

Table 4.1: Sensitivity analysis of particle diameter and injection location (Stovin and Saul, 1998).

Run	1	2	3	4	5	6
Injection Location	Horizontal			Vertical		
Diameter [μm]	28	47	88	28	47	88
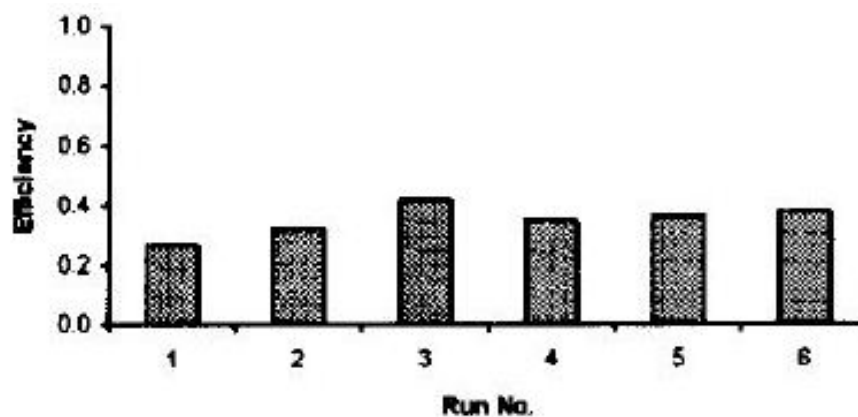
Figure 4.7: Sensitivity analysis of particle size and injection location (Stovin & Saul, 1998).

Dufresne *et al.* (2009) found that the solution was sensitive to density due to one of the main term in the settling process $g\frac{\rho_p-\rho}{\rho_p}$. Stovin and Saul (1998) found that the separation efficiency was less sensitive to density for high velocities, figure 4.8.
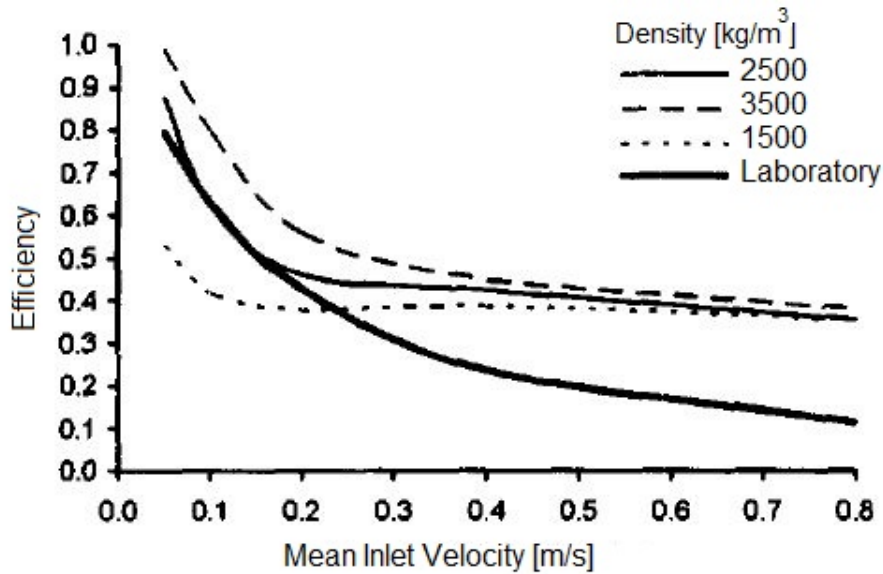
Figure 4.8: Sensitivity analyzes of particle density (Stovin and Saul, 1998).

4.2.5 Boundary Conditions for the Discrete Phase

Boundary conditions must be defined for walls, bed, inlet, outlets and overflows of the geometry. The accuracy of predictions of separation efficiency and deposition locations is dependent on how well the boundary conditions are set.

4.2.5.1 Default Boundary Conditions

The default boundary conditions that are available in FLUENT are *trap*, *escape*, , *saltate*, and *reflect*, table 4.2 (ANSYS Inc., 2010a).

Boundary type	Description
Trap	The particle is terminated and sticks to the surface
Escape	The particle terminates at the boundary and is vanished
Saltate	The particle is placed in a small distance from the wall to avoid "trickling" along the wall
Reflect	The particle rebounds from the boundary

Table 4.2: Description of default boundary conditions (ANSYS Inc., 2010a).

When studying sediment transport *escape*, *reflect* and *trap* are suitable at inflow, outflow and wall boundaries. The physics associated with the particle deposition, however, is complex and difficult to model. The following section therefore discusses the boundary condition at the bed of the CSO chamber.

The *trap* condition terminates particle trajectories at the first contact with the boundary. Stovin and Saul (1998) found that this overestimated the separation efficiency, figure 4.9. The deviation between experiments and CFD simulations are most significant for high velocities. This can be explained by the dynamic behavior of particles where the bed load roll and slide along the bottom and are eroded after they have settled.
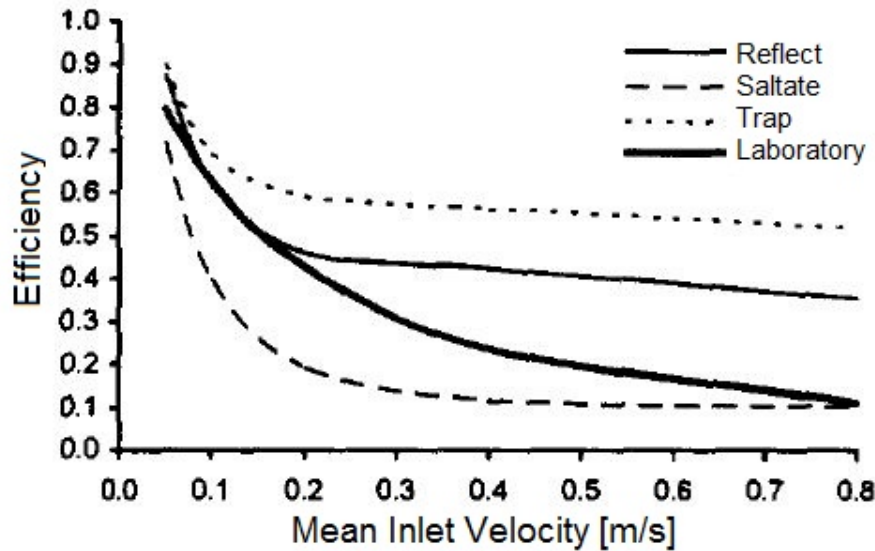
Figure 4.9: Sensitivity analysis of boundary conditions (Stovin & Saul, 1998).

Stovin and Saul also investigated the *reflect* boundary conditions and included a limit for how many times a particle could be reflected before it settled (1998). This gave better results, but was not recommended due to high sensitivity to cell size close to the boundary. Further, it did not have a physical meaning and was not correlated to the hydraulics.

4.2.5.2 Bed Shear Stress (BSS)

When the default boundary conditions do not give trustworthy results a user defined function (UDF) must be made. Adamsson, Stovin and Bergdahl developed a bed shear stress (BSS) boundary condition (2003). When the local bed shear stress in a cell was lower than a critical bed shear stress value the particle was trapped, otherwise it was reflected. Comparisons with laboratory work showed good correlation for this boundary condition with regards to both trap efficiency and location of depositions. The critical value for bed shear stress used was 0.004 Pa for study of a sedimentation basin.

Dufresne *et al.* (2008) investigated the BSS boundary condition further with different flow conditions. For a tank with low water depth the flow field was characterized by one large circulation. Deposit locations with BSS showed good correlation with laboratory results. When the same geometry was studied during overflowing with consequently higher water depth, the flow pattern consisted of two quasi-symmetrical large circulations. The BSS condition where not in agreement with experimental data. Another boundary condition that considered the bed turbulent kinetic energy (BTKE) was then tried. This method gave satisfying results for the case with high water depth and a threshold of 0.00015 $\frac{m^2}{s^2}$. This study concluded that the threshold value for the boundary condition was very important.

Chapter 5

Modelling of Open Channel

5.1 Problem Description

This is a study of a rapid insufficient open channel flow over a step. It is a 10m long flat channel with a 0.25m high step in the middle, figure 5.1 In numerical modelling it is important to start with simple cases, to test different modelling approaches relatively fast. The purpose of the modelling of a simple channel is to validate the model and investigate the possibilities in the DPM model. The methodologies found here should be the foundation for modelling of a CSO in chapter 6.
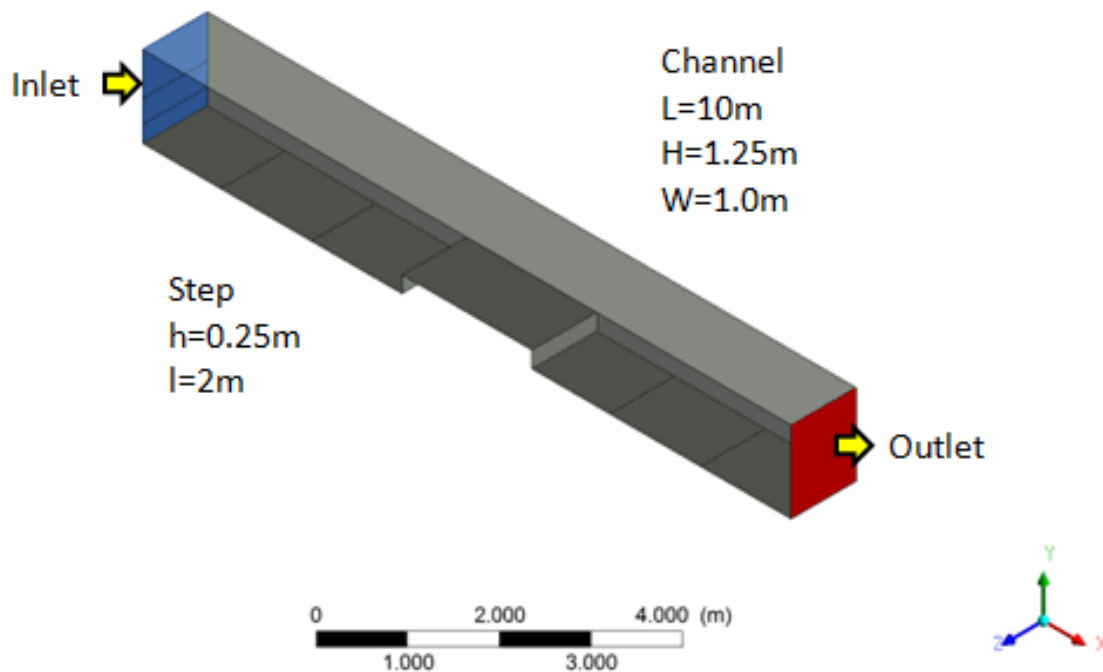
Figure 5.1: Geometry of the channel modelled.

5.2   Computational Grid

Design modeller was used to create a hexahedral mesh with 270270 elements. Local refinements where made in areas where it was important to capture the flow field. An inflation layer was created close to the wall, figure 5.2, and cell size control was applied around the corner of the step, figure 5.3. The mesh was also refined in FLUENT before each iteration 15cm under and above the initial water level specified by the user.
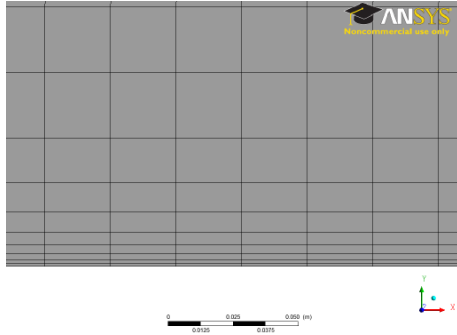
Figure 5.2: Inflation layer close to wall.
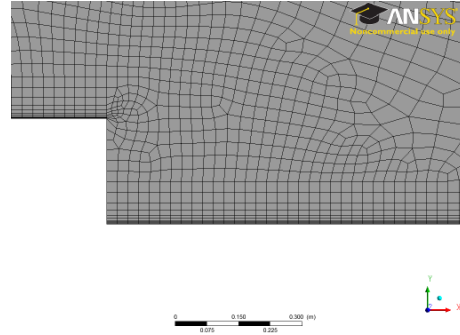
Figure 5.3: Refinement of mesh around corner.

The quality of the mesh can be measured in terms of skewness where 0 is excellent quality and 1 is bad quality. The mesh in the channel had a good quality with an average skewness of 0.07. The few bad elements were located at the corner of the step.

5.3   Set-up

Time varying, $transient$, simulations were set-up with a pressure-based solver. The flow regime can be characterized as a stratified or free-surface flow because it is a clear interface between the two phases, and the volume of fluid (VOF) method with open channel boundaries was applied. Air was chosen as the primary phase and water as the secondary phase in the VOF model. The surface tension between the phases was set to $0.072N/m^2$. The open channel flow boundary condition was applied and the initial water level was set to 0.5m. The boundary condition at the inlet was mass flow inlet, and mass flow rate was defined for each phase. Mass flow rate is the product of the velocity of the fluid, area and density ($\dot{m} = \rho v A$). The air mass flow rate was set to 0 kg/s and the mass flow rate of water was set to 1500 kg/s. This means that the velocity is 3.0 m/s. The outlet was set to an outflow boundary with flow rate weighting 1 because there is only one outlet.

The DPM model was applied for the particle tracking. It was assumed that the flow field was not disturbed by particles, and an uncoupled approach was performed. The step length factor was 20 and the number of time steps was set to 50 000. Particle tracks where based on a converged flow field in a steady state manner. Inert type of particles where injected uniformly from the inlet. A mass flow rate of 10 kg/s of sand particles with density 2650 kg/m^3 and diameter 1mm was injected. The trap condition was used at the bed boundary. This was done since the purpose was to identify possible methodologies for analyzing of sediment transport. Separation efficiency would be studied in the real CSO in chapter 6.

5.4 Validation of Flow Field

Particle tracks are calculated based on the flow field. It is therefore of great importance that the flow field is validated so one can rely on the results. Validation in the field of CFD is defined as (Slater, 2008) "The process of determining to what degree to which a model is an accurate representation of the real world from the perspective of the intended uses of the model." This will be illustrated in this section with validation of the predicted water surface level of the open channel flow. The methodology for reviewing turbulence models will also be shown.

5.4.1 Water Surface Prediction

5.4.1.1 Theoretical Water Level Calculations

This section compares the free surface profile of a numerical simulation with theory. The flow phenomena studied is an an insufficient rapid flow as shown in figure 5.4 (Ugarelli, 2011). The relationship between water depth and specific energy is given in equation 5.4 (Crowe, Elger & Roberson, 2005).
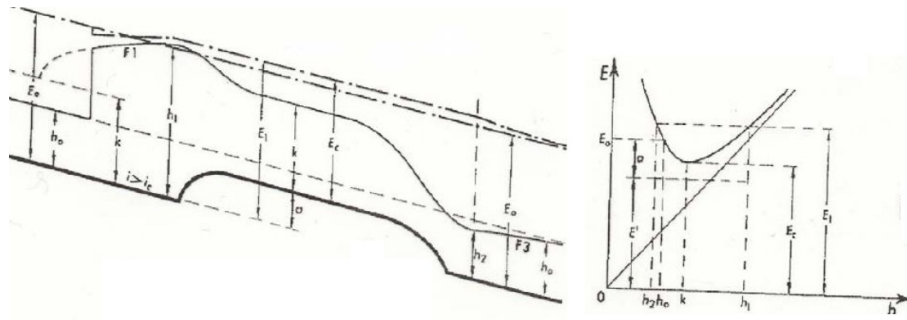
Figure 5.4: Theoretical profile to be obtained and specific energy vs. depth (Ugarelli, 2011).

To be able to validate the model, the theoretical water depths had to be found for the specific case. The initial water depth, y_1, was set to 0.5m, and the velocity was 3m/s which gave a mass flow rate of 1500 kg/s. The critical depth is defined when Fr=1 and is uniquely determined by the discharge in the channel according to equation 5.1. The critical energy in the channel could then be determined by 5.2. To find the highest and lowest depths, y_1 and y_2, it was necessary to calculate the minimum energy that was required to push water over the step, equation 5.3. When the specific energy level was known, the depths y_1 and y_2 could be found with goal seek of equation 5.4 in EXCEL. The depths and corresponding specific energy calculated based on theory for the modelling case is shown in figure 5.5.

$$Fr = \frac{v}{\sqrt{gy}} = \frac{Q}{\sqrt{gy}A} \tag{5.1}$$

$$E_c = \frac{3}{2}y_c \tag{5.2}$$

$$E_{min} = E_1 = E_c + a \tag{5.3}$$

$$E = y + \frac{q^2}{2gy^2} \tag{5.4}$$

27
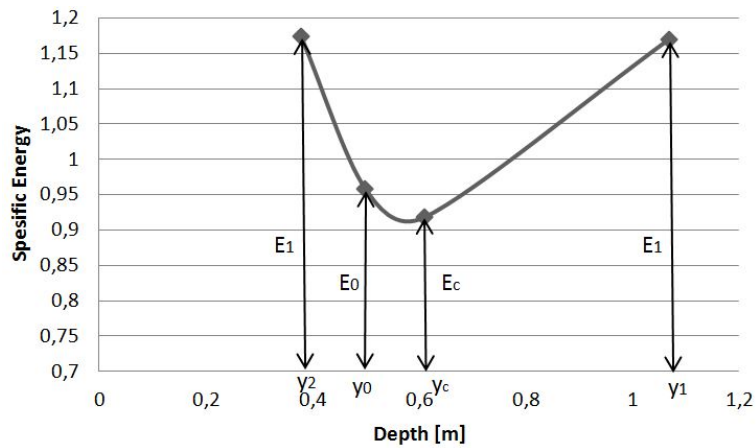
Figure 5.5: Water depth and specific depth from calculations of the specific flow scenario.

5.4.1.2 Modelled Water Level

The water surface profile obtained after convergence of the model is shown in figure 5.6. The surface is coloured by velocity. After the inlet the flow is supercritical due to the high velocity 2m/s and low water depth 0.5m. About 2 m before the step the flow becomes subcritical as the velocity is reducing and the water depth is rising. This is because there must be sufficient static head to push the water over the step. Over the step the flow is increasing the velocity and becomes supercritical. After the step there is a hydraulic jump where the flow becomes subcritical. Energy is then lost, and this is why this is called an insufficient flow.
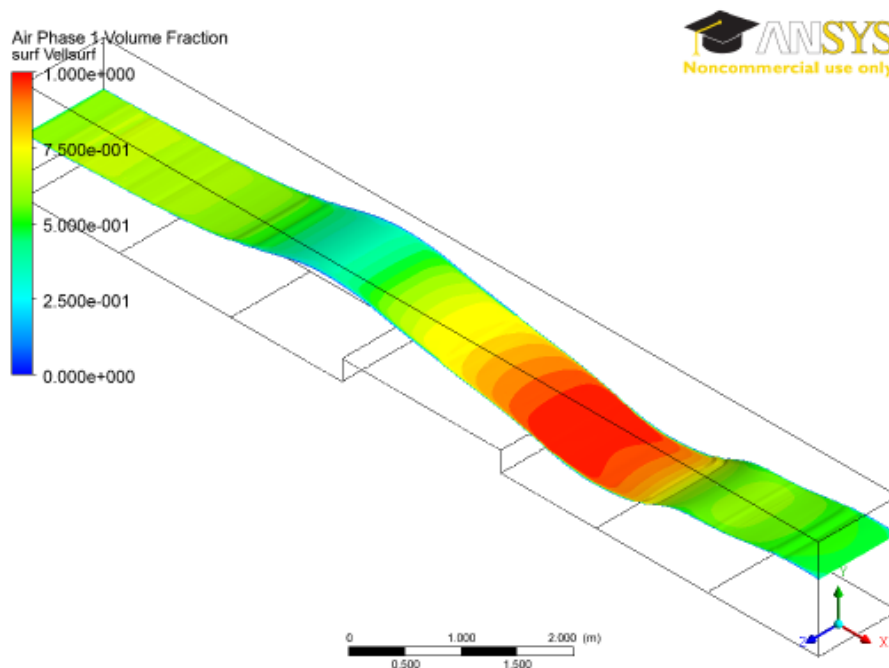
Figure 5.6: Water surface profile colored by velocity.

The shape of the surface had the right profile, but the predicted water depths must be compared to the calculated depths shown in figure 5.5 to be sure that the modelling is correct. The figure shows very good correlation between the water depths predicted and the values expected from calculations.
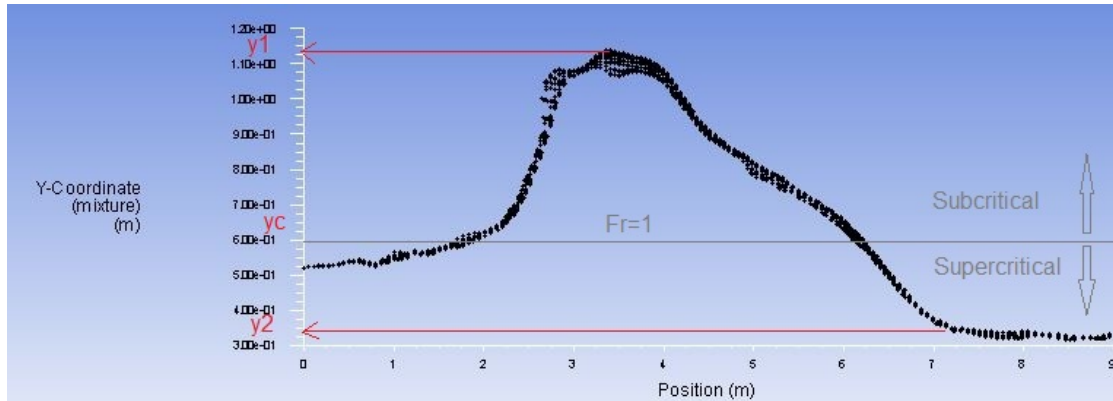
Figure 5.7: Modeling results for water depth vs. distance from inlet.

5.4.2 Turbulence Model

Turbulence modelling is important as the direction of the velocity vectors often have an effect on the particles. After the step a recirculation zone occurs as seen from figure 5.8. The reattachment length is a widely used parameter to validate the turbulence. In this case study the k-ε method was applied. The reattachment length after the step was found to be 0.66m ($2.64H_{step}$) by plotting wall shear stress, figure 5.9. No experimental data where available for comparison, so no further assessment was done. It should be noted that the re-attachment length is a function resolution of the mesh, the Reynolds number and the turbulence model.
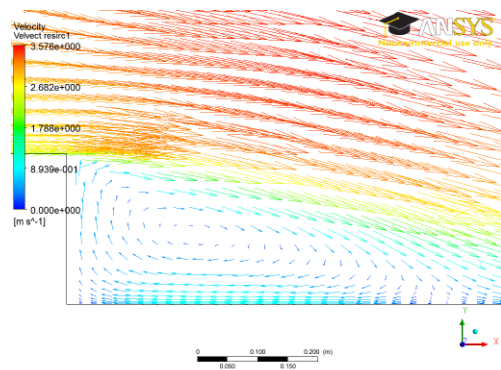
Figure 5.8: Recirculation after step.
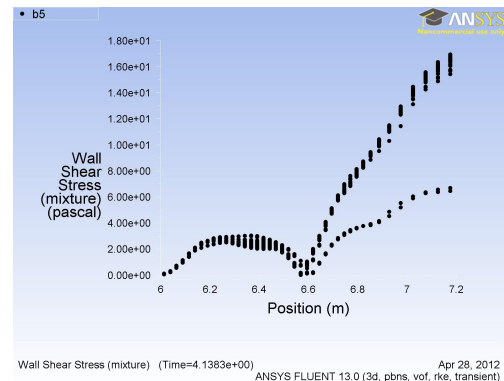
Figure 5.9: Wall shear stress for recirculation zone.

5.4.3 Near Wall Cell Size

Chapter 4.1.1 discussed the importance of capturing the laminar sub layer close to the walls. The $y+$ value is used as a parameter to decide if a suitable wall turbulence model is used. The correlation between height of cell, y, and y^+ is illustrated in equation 5.5.

29

$$y = \frac{y^+ \mu}{U_\tau \rho} \tag{5.5}$$

This can be used to make an estimate for what the cell size should be close to the wall. An input parameter is the shear velocity, U_τ, which can be calculated from equation 5.6. It is a function of the wall shear stress, τ_w, equation 5.7. To calculate the wall shear stress the Reynolds number and skin friction must be found respectively from equation 5.8 and equation 5.9. This procedure was used to find the cell size required to obtain $y^+ = 70$. This resulted in a cell size height y=1mm.

Shear velocity, U_τ:

$$U_\tau = \sqrt{\frac{\tau_w}{\rho}} = \sqrt{\frac{6.0N}{1000 \frac{kg}{m^3}}} = \underline{0.078 \frac{m}{s}} \tag{5.6}$$

Wall shear stress, τ_w:

$$\tau_w = \frac{1}{2} C_f \rho V^2 = \frac{1}{2} \cdot 1.92 \cdot 10^{-3} \cdot 1000 \frac{kg}{m^3} \cdot (2.5 \frac{m}{s})^2 = \underline{6.0N} \tag{5.7}$$

Reynolds number, Re:

$$Re = \frac{\rho V L}{\mu} = \frac{1000 \frac{kg}{m^3} \cdot 2.5 \frac{m}{s} \cdot 10m}{10^{-3} \frac{kg}{ms}} = \underline{2.5 \cdot 10^7} \tag{5.8}$$

Skin friction, C_f:

$$C_f = 0.058 Re^{-0.2} = 0.058 \cdot (2.5 \cdot 10^7)^{-0.2} = \underline{1.92 \cdot 10^{-3}} \tag{5.9}$$

The inflation layer close to the wall was made with a refinement of 1mm according to the calculations above. The y+ values when the solution had converged was then plotted in figure 5.10. The mesh is satisfying when $30 < y^+ < 300$ for the standard wall function. Figure 5.10 shows that all the y+ values are below 70 which is good. Before and after the step ($2m < x < 4m$ and $6m < x < 6.6m$) the y+ values are too low. This can be explained as a result of the slow velocity in these regions. Based on the y+ values one can conclude that the resolution of the cells is high enough and the right near wall turbulence model is applied.
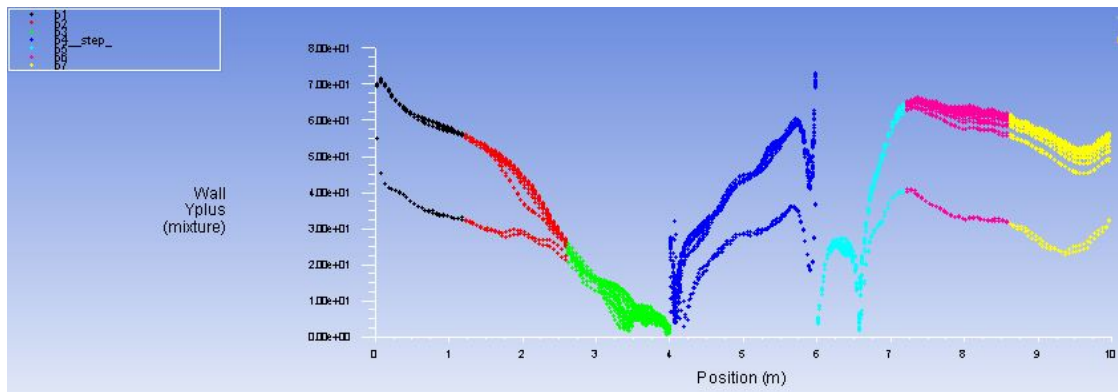
Figure 5.10: Wall y+ values.

5.5 Results from Particle Tracking

This section demonstrates what information that can be obtained with the particle tracking model. The simple geometry served as a testing environment to show possibilities for particle tracking and the objective was thus not on obtaining any specific results.

5.5.1 Particle Trajectories

Particle tracks are the predicted trajectories that show how the particles will move in the fluid. Particle trajectories can be coloured by a variety of parameters such as velocity magnitude, diameter, particle Reynolds number and number of particles in parcels. The most widely used parameter is, however, the particle residence time. It gives information about still zones and recirculation zones. Figure 5.11 illustrates particle tracks for different particle sizes coloured by residence time. The largest particles with diameter 5mm all sink to the bed before the step, while some of the 2mm particles flow over the step. The particles with diameter 1mm are suspended in the fluid until after the step where all of them sinks to the bed. All the particle tracks show that particles are trapped in the area before the step. Here the residence time is high, which means that they are trapped in this region.
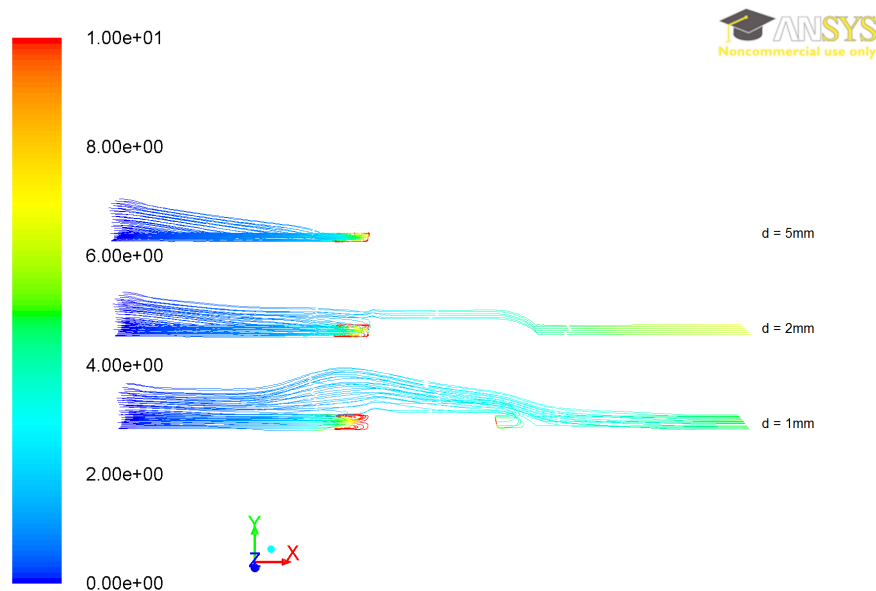
Figure 5.11: Particle tracks coloured by residence time, d = 5mm, 2mm and 1mm.

5.5.2 Final Location of Particles

When particle trajectories are calculated the final position, *fate*, of the particle is reported as escape or trap. The number of particles within each category is reported and this can be used to calculate the separation efficiency. There was no need to calculate the separation efficiency in the channel since it is not a combined sewer overflow. In addition to the total number of particles within each fate, one can obtain a summary report for each boundary zone. The bed was divided into several boundaries, figure 5.12, to get information about the number of particles settled in each section. Additional information from the summary report is the time until the particle reaches its reach its final destination, *residence time*. A typical summary report is illustrated in figure 5.13.

ID	5	6	7	8	9	10	11
Boundary	B1	B2	B3	B4 (step)	B5	B6	B7
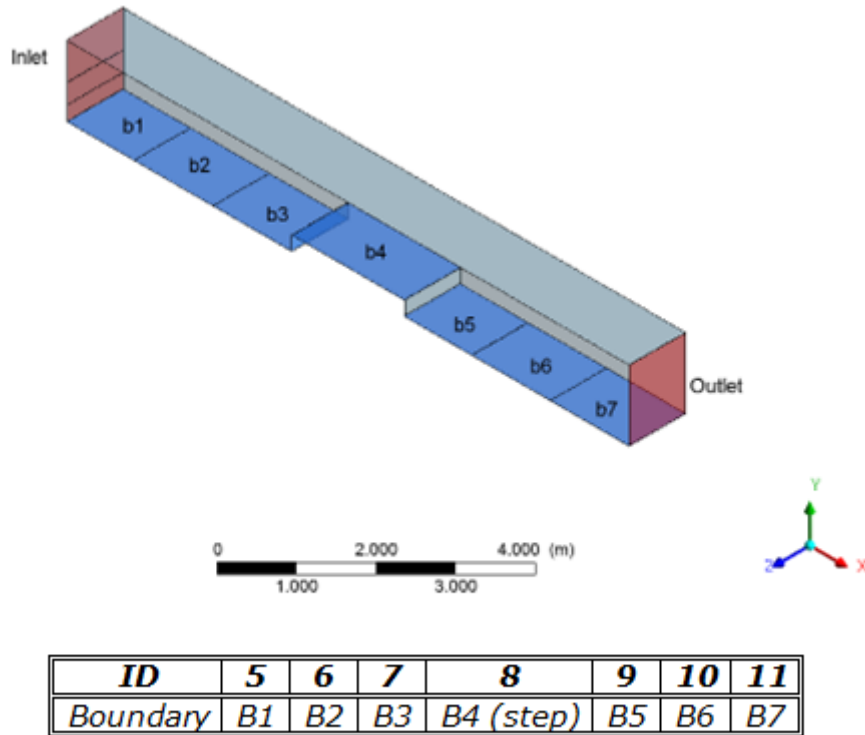
Figure 5.12: Boundary zones at the bed of the channel.

```
Fate                Number          Elapsed Time (s)
                                 Min        Max        Avg       Std Dev
----                ------    ---------- ---------- ---------- ----------
Trapped - Zone 5      282    1.609e-02  4.365e-01  1.144e-01  9.418e-02
Trapped - Zone 6       70    4.389e-01  9.345e-01  5.781e-01  1.336e-01
Trapped - Zone 7       68    1.083e+00  2.762e+00  1.696e+00  5.287e-01
Trapped - Zone 8       71    2.385e+00  4.355e+00  2.611e+00  2.859e-01
Trapped - Zone 9       34    3.281e+00  3.668e+00  3.328e+00  8.319e-02
Trapped - Zone 10      70    3.353e+00  4.138e+00  3.522e+00  1.580e-01
Trapped - Zone 11     105    3.734e+00  4.883e+00  3.946e+00  2.084e-01
```

Figure 5.13: Summary report for final destination of particles.

The spatial distribution of particles is important to identify settling zones where one should expect accumulation of sediments. A particle deposition plot could be made to visualize the point of impact where particles are trapped, 5.14. The plot shows that many particles are trapped at the inlet, and this is because they are registered as trapped at the first contact with the bed. It is not the result of this plot that is of importance, but the principal of how post-processing can be done.
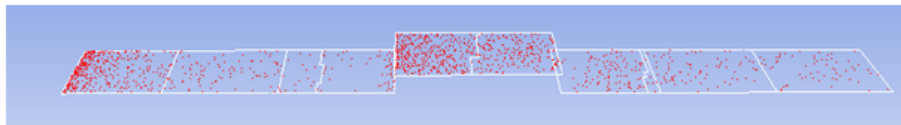
Figure 5.14: Particle deposition location.

The post-processing of the DPM model has shown the capabilities of the model which are the basis for modelling of sediments in the CSO.

Chapter 6

Modelling of Complex CSO

6.1 Problem Description

6.1.1 CSO Geometry and Mesh

A CSO in Århus in Denmark was utilized as a practical application to study the quality performance of a CSO. The CSO was a complex structure with one inlet (A=$4m^2$), 4 rectangular overflows (A=$2m^2$) and 2 outlet pipes (A=$0.8m^2$), figure 6.1. The sewage is entering the CSO through a rectangular inlet and flows in to a curve with approximately 45 degrees, figure 6.2. There is a drop in the bed of the CSO chamber and a flow divider between the outlet pipes.
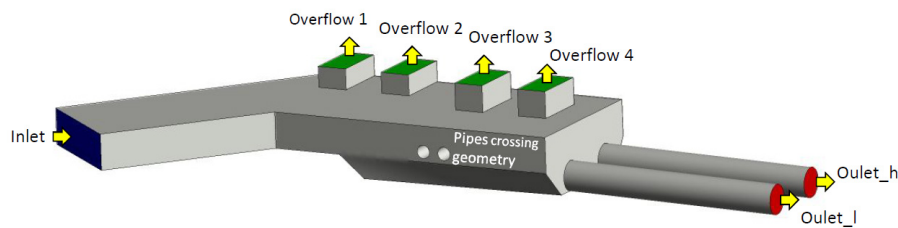
Figure 6.1: Århus geometry - top inner side perspective.
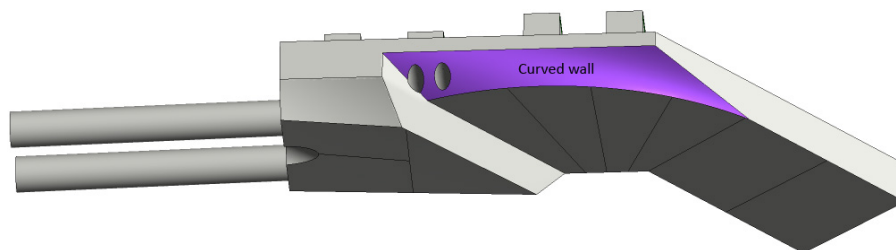
Figure 6.2: Århus Geometry - bottom outer side perspective.

A tetrahedral mesh was applied to the main body of the CSO chamber, while hexahedrals where used for the overflow structures. The total number of mesh elements were 400 000. A quick check of the mesh showed a good quality with skewness 0.22 and orthogonality 0.86. A grid independence test was not done, as the grid had a satisfying quality.

6.1.2 System Description

The operation of a CSO must be seen as a part of the sewer system and not as an isolated device. The location of the CSO has an important role in time of operation and how well the separation degree is. In Århus the case study CSO is located in conjunction with a waste water treatment plant (WWTP) and is connected to a detention basin, figure 6.3. The WWTP receives sewage from Åby and Åby vest. When the capacity of the treatment plant is reached, the excess water is transferred in a 130m long channel and into the CSO. After the CSO there is a detention basin that should reduce the number and magnitude of CSO spills. When the WWTP has capacity left, sewage from the basin can be pumped back and treated. The flow that goes into the WWTP and through the filter house is crossing the CSO geometry. This is why there are two pipes that go through the geometry in figure 5.1. Even though they are not a part of the CSO, they must be included as they will effect the flow field.
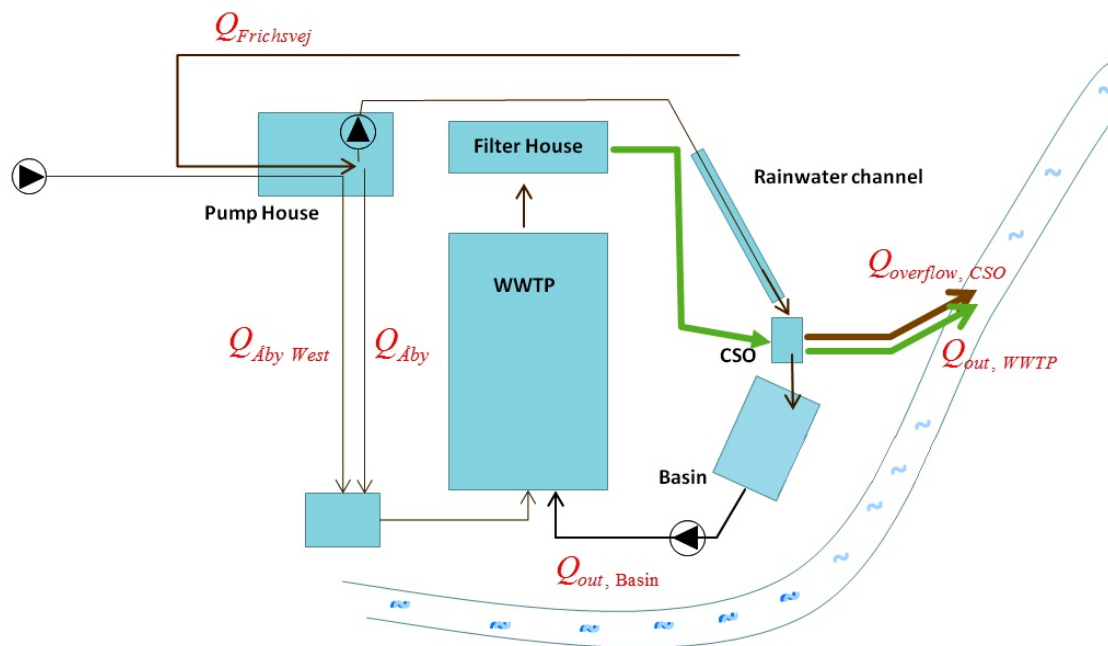
Figure 6.3: System drawing (Skjetne, 2012).

If the capacity of the basin and treatment plant is exceeded, the CSO is overflowing. First, overflow 1 and 2 start to function and an alarm alert that sewage is discharged to the receiving waters, figure 6.4. 15 cm above this level the other CSOs start to overflow.

Figure 6.4: CSO overflow with alarm (Photo: Anders-Lyggard Jenssen & Lars Hem).

6.1.3 Flow Data and Modelling Scenarios

Water level measurements collected during one month, August 2011, where used to determine the flow scenarios that should be modelled. Water level was measured at three locations, in the upstream channel and in the CSO and basin as illustrated in figure 6.5. A longitudinal profile of the system with water level reference heights and the main dimensions are illustrated in figure 6.6 (Skjetne, 2012). The change in water level in the basin was used to calculate the inflow discharge [l/s] to the basin.
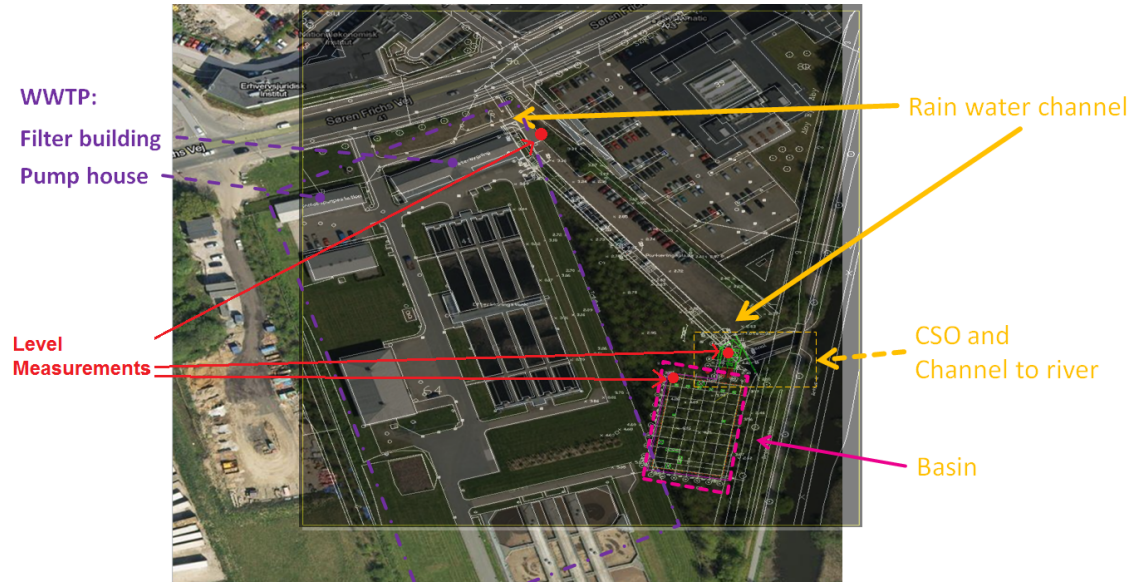
Figure 6.5: The location of the CSO in the system (Skjetne, 2012).
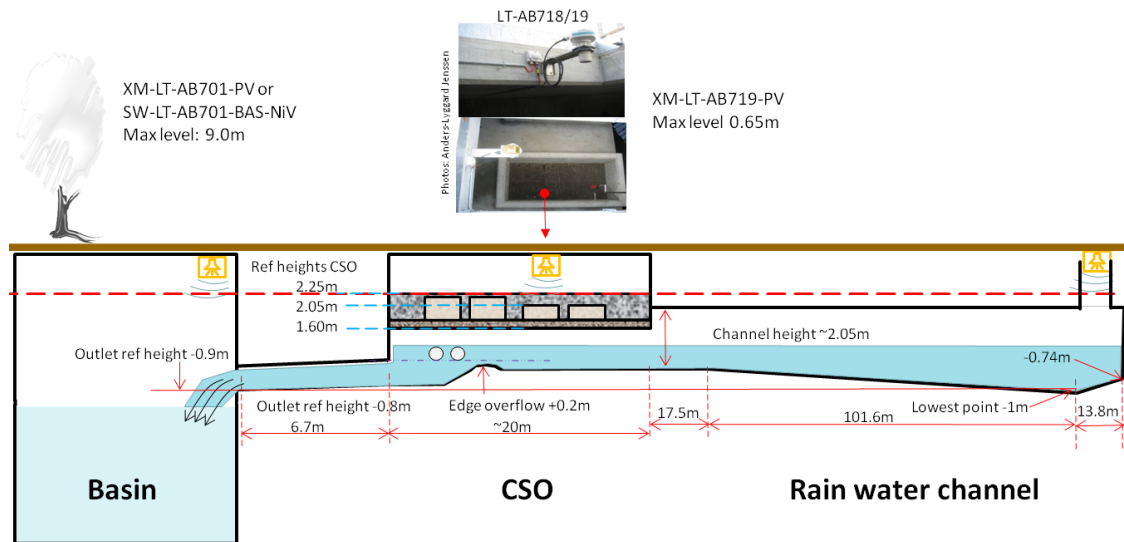
Figure 6.6: Longitudinal profile (Skjetne, 2012).

The highest flow event that occurred during August 2011 (20.08.2011) was chosen as the modelling scenario. The measurements from this period is shown in figure 6.7. The water level measurement in the basin and CSO where used to calculate the volume change in flow rate. Time varying boundary conditions at the inlet will not be included as this is extremely difficult to model. The effect of variations in flow will, however, be tested by modelling different velocities and different degree of filling. The maximum flow velocity from this event was found to be approximately 0.7 m/s, so this was used as the maximum velocity that was used in the modelling.
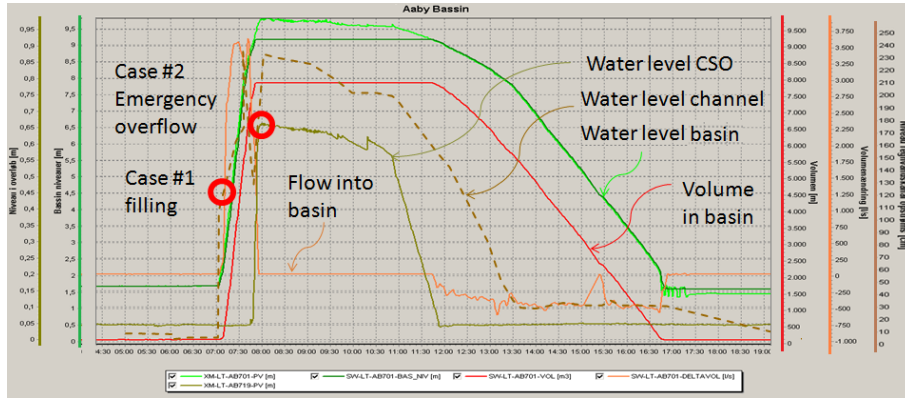
Figure 6.7: Water level measurements from the largest flow event during August 2011 (Skjetne, 2011).

In the first stages of the storm event, the water level in the channel increases and the basin is starting to fill. When the water level in the basin reaches 9m the volume is approximately $6000m^3$ and the basin is full. This causes an increasing water level in the CSO. This situation is the basis for the first modelling scenario of the CSO as it is interesting to study the sediment transport during a storm event before the device is overflowing, right side 6.8.

The water level recorded in figure 6.7, is measured with the roof of the CSO chamber as a reference level and gives the water height in the rectangular overflow structures. When the measured water level is 0.65m the CSO is in overflow mode. This is the second scenario, left side figure 6.8, that should be modelled numerically as it is of interest to estimate the separation efficiency of sediments.
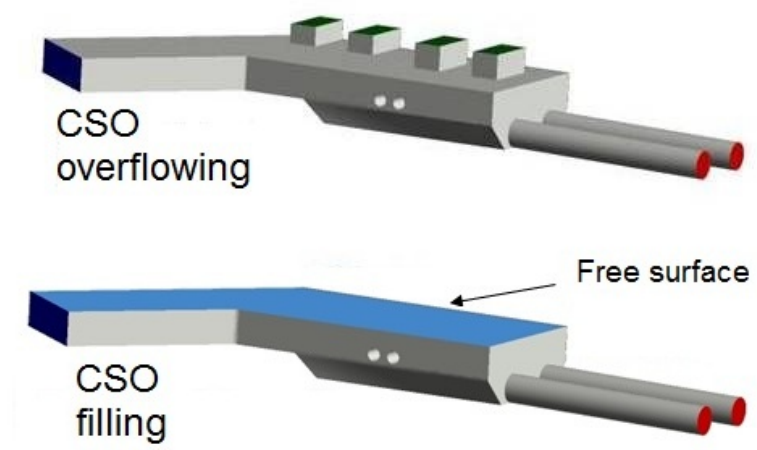
Figure 6.8: Modeling scenarios.

6.2 Set-up of Simulations

6.2.1 Solver

The general set-up of solvers was the same as for the simple channel, chapter 5, and will not be discussed in more detail here.

6.2.2 Boundary Conditions

Boundary conditions were set up for the continuous phase (fluid) and the discrete phase (particles).

6.2.2.1 Boundary Condition for the Continuous Field

A velocity inlet was applied for velocities of 0.3m/s, 0.5m/s and 0.7m/s. A fully developed velocity profile was used as shown in figure 6.9. The velocities close to the walls are slowed down by friction and the highest velocities are in the middle of the inlet. Appendix 3 contains the UDF that was applied to create a fully developed profile for a square inlet and is based on equation 6.1 and 6.2 from White (2006). It is important that the coordinate system lies in the center of the inlet as y is the width of the channel and is in the interval $-a \leq y \leq a$ and z is the height in the interval $-b \leq z \leq b$. The pressure gradient, $\frac{d\hat{p}}{dx}$, was calculated for different discharge values, Q, in Excel, appendix 3.

$$u(y,z) = \frac{16a^2}{\mu\pi^3}(-\frac{d\hat{p}}{dx}) \sum_{i=1,3,5}^{\infty} (-1)^{(i-1)/2}[1 - \frac{cosh(i\pi z/2a)}{cosh(i\pi b/2a)}] \times \frac{cos(i\pi y/2a)}{i^3} \tag{6.1}$$

$$Q = \frac{4ba^3}{3\mu}(-\frac{d\hat{p}}{dx})[1 - \frac{192a}{\pi^5 b} \sum_{i=1,3,5}^{\infty} \frac{tanh(i\pi b/2a)}{i^5}] \tag{6.2}$$
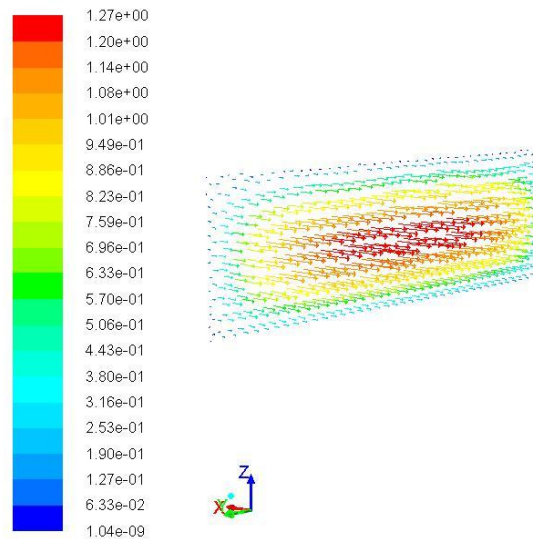
Figure 6.9: Fully developed velocity profile for square inlet.

In the overflow scenario pressure outlets were used at the overflow chambers and the outlets was set to

walls as the basin was full. During filling of the CSO the pressure outlets was used for the pipes through the treatment plant. A free surface was modelled as a friction free wall, right side in figure 6.8. The free surface level was predefined by the user. As the modelling of the channel showed there are change in water level dependent of the energy level. It is therefore a simplification to assume that the surface is horizontal. But since the flow velocity is relatively low and the water depth is high during overflow. The flow would be subcritical so the assumption would give a little deviation from a free surface.

Turbulence was specified by turbulent intensity in percentage and hydraulic diameter for both for all the flow boundaries.

6.2.2.2 Boundary Conditions for the Discrete Phase

The BSS boundary condition is applied in the study of the CSO in Århus as this is the boundary condition that has physical meaning and captures the problem. Chapter 2.2.3 showed that an appropriate threshold value for deposition in a combined sewer would be 1.0 Pa.

6.2.3 Particle Injections

This study should investigate the quality aspect of the CSO performance and is a conceptual study of typical sediments. The flow data where collected at the cite location in Århus, while typical sewer sediments where found from literature, see section 2.1.4, and where not based on sampling. The particle densities operated with where 2650 kg/m^3, 2000kg/m^3, 1720kg/m^3, 1400kg/m^3, 1170kg/m^3 and 1002kg/m^3. Further investigations were needed to find the particle sizes that would be affected by the flow conditions.

A first indication was found by using the flow field with inlet velocity 0.7m/s and trap boundary condition. The results shown in figure 6.10 are not statistically consistent results as only one injection for each particle type was tested. The reason for this was that this served as a preliminary investigation of particle sizes and where not the final separation efficiency results. This method gave a coarse categorization of particles that gave the limits for particles to be modelled, figure6.10. Particles that where expected to give a separation efficiency of nearly 100% (all sedimented) or 0% (all suspended) where not of interest. The largest particles that should be considered were floaters with a density of 1002 kg/m^3 and diameter 5mm. Particles with larger diameters where sedimented independent of particle densities. The smallest particles that where practical to model was found to be particles of 100μm.
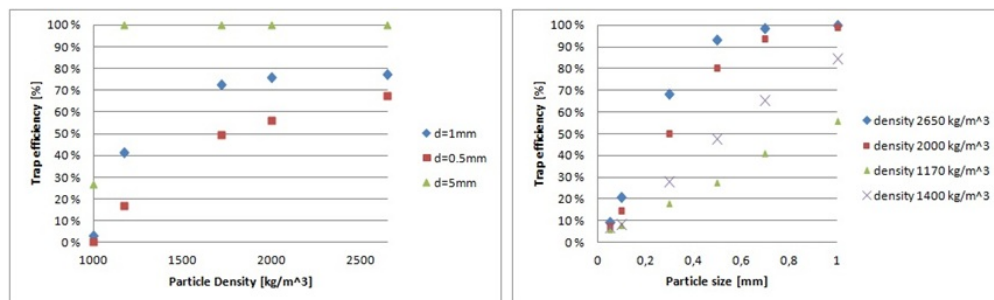
Figure 6.10: Preliminary investigation of the influence of particle size.

750 particles of each particle type was distributed uniformly over the inlet. The effect of turbulence was included by 10 stochastic tries for the RWM. The initial velocity of the particles was assumed to be the same as the fluid velocity. The mass flow rate for each fraction was 10kg/s and the step length factor for the simulation was set to and 50 000 time steps. Coupling between the DPM model and fluid field was used and a steady particle tracking approach was applied.

6.3 Flow Results

First, the results from the flow field are presented as this is the basis for the particle tracking. Results are shown for an inlet velocity of 0.7 m/s and post-processed on surfaces according to figure 6.11. Contour plots of velocity, streamlines and bed shear stress were examined during filling of the CSO and overflow to receiving waters. The results for both scenarios are presented first followed by a discussion where the observations are interpreted.
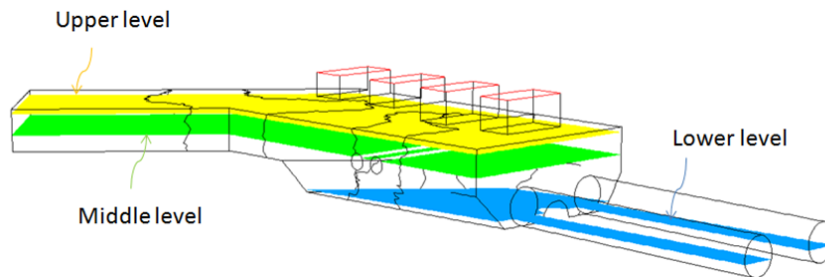
Figure 6.11: Cross sections for post-processing of results for fluid field.

6.3.1 Scenario 1 - Filling of CSO

6.3.1.1 Contour Plots of Velocity Magnitude

Figure 6.12 shows velocity magnitude at three water depths. Following observations where done:

- The profile evened out after the inlet and maximum velocity decreased;

- The main flow moved towards the inner side of the CSO in the bend and created an area with low velocity on the outer side of the curve;

- A tranquil area was observed at the back edge of the inner corner; and,

- The flow had lower velocities when the depth was increased.
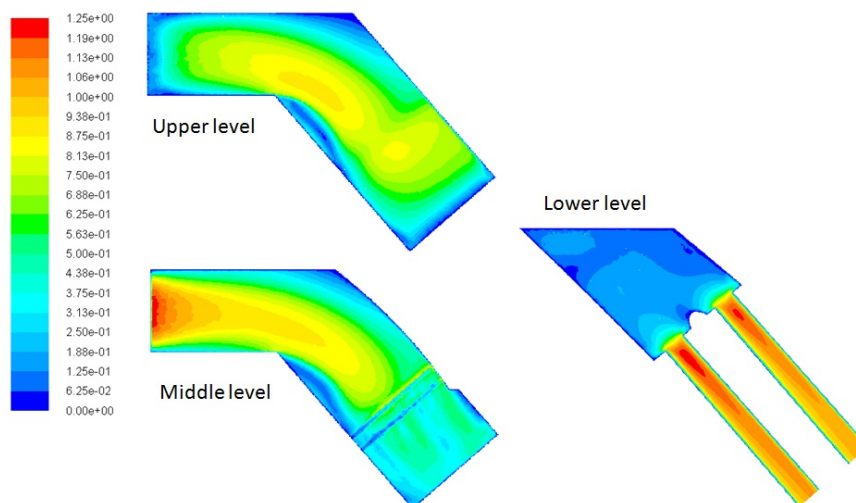
Figure 6.12: Comparison of contour plots overflowing and filled CSO.

39

6.3.1.2 Flow Streamlines

Velocity magnitude alone is not enough to study, as direction of the flow is of great importance. Stream-lines are used to describe the movement of the flow. Figure 6.13 shows streamlines coloured by residence time which is the period the fluid particle uses through the domain. The following observations where done:

- Streamlines injected from the middle and upper part of the inlet had direct paths to the outlets without any major rotations;

- The flow injected from the bottom part of the inlet obtained a clockwise rotation after the step. It had a lateral movement towards the outer side of the CSO and escaped through the left outlet; and,

- The residence time for the bottom streamlines to the right outlet was halved compared to the left outlet.
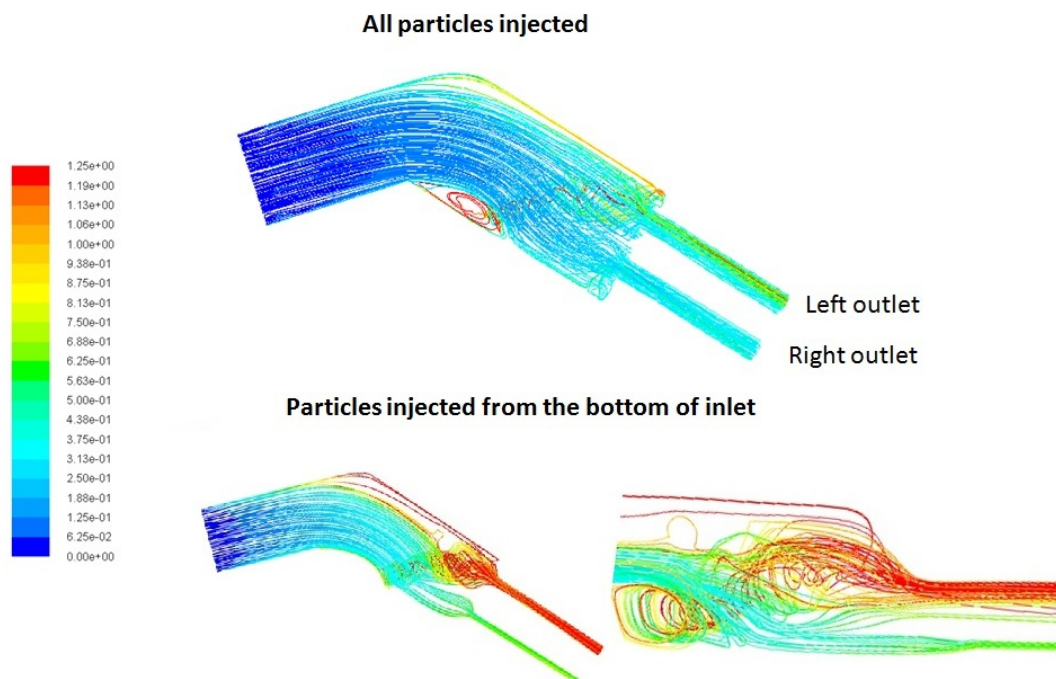
Figure 6.13: Streamlines during filling of CSO.

6.3.1.3 Bed Shear Stress

This will be presented in a comparison of the filled and overflow scenario in the discussion, section 6.3.3.

6.3.2 Scenario 2 - Overflow of CSO

6.3.2.1 Contour Plots of Velocity Magnitude

Figure 6.14 shows contour plots for the CSO and the characteristics of the flow field is summarized in the following:

- The flow advanced along the outer wall in the curve;

- Water was pushed out of the overflows 1-3 as seen from the increase in magnitude in the upper level;

- A tranquil area was identified at the inner part of the CSO after the bend; and,

- After the drop in bed level there was a region with low velocities as seen in the plots from all depths.
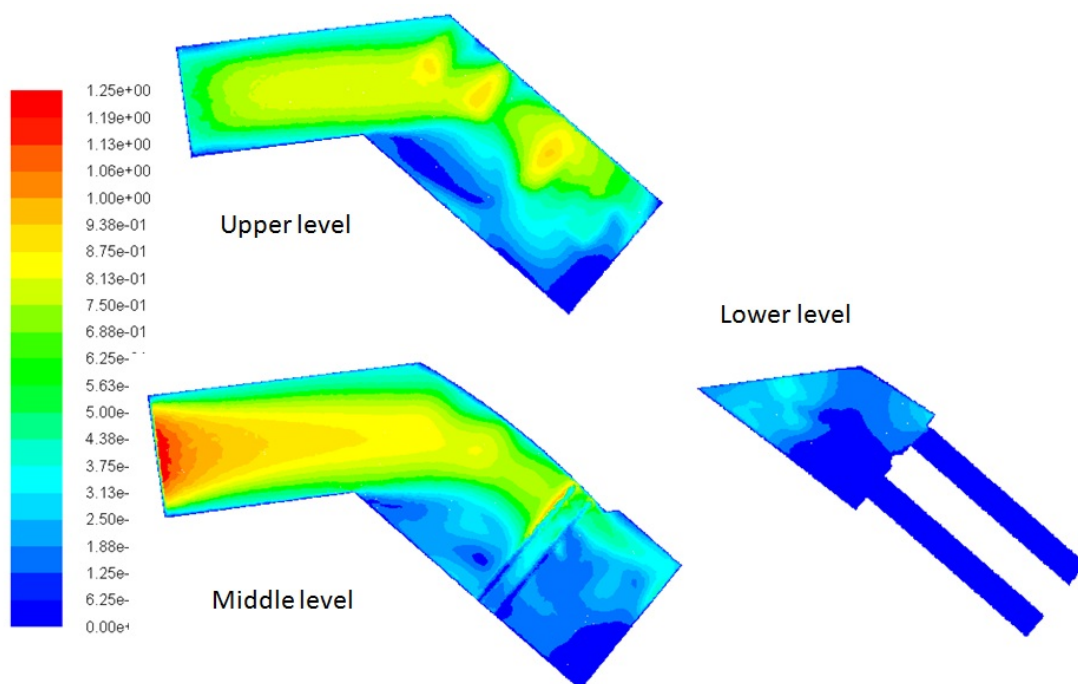
Figure 6.14: Horizontal velocity contour plots.

6.3.2.2 Flow Streamlines

The CSO during overflow has a complicated flow pattern, figure 6.15, which is best understood when looking at a perspective from the side and above simultaneously. The main trends are summarized based on the inlet location right, middle and left side:

- Least flow, 16%, escaped through overflow 3, followed by 25% in overflow 2 and 28% in overflow 1. Overflow 4 had the largest fraction of the flow rate with 31%;

- The inlet region had nearly parallel streamlines;

- Streamlines originated from the left side escaped through overflow 1;

- Streamlines originated from the right side of the inlet reached the step in the middle of the section. After the step a large clockwise rotation was created. Also a part of the flow that moved over the crossing pipes where dragged down into the rotation. The streamlines where leaving the recirculation zone above the pipes. Some escaped directly through overflow 3 and 4, while others hit the wall at the end of the chamber and had another rotation before they reached overflow 4;

- The flow injected at the middle on the right side followed the outer curve of the CSO and escaped through overflow 2 or overflow 4; and,

- Streamlines from the middle on the left side obtained s-shaped streamlines with a rightward movement after the curve followed by a leftward motion into overflow 4.

Figure 6.15: Streamlines for overflow coloured by residence time.

42
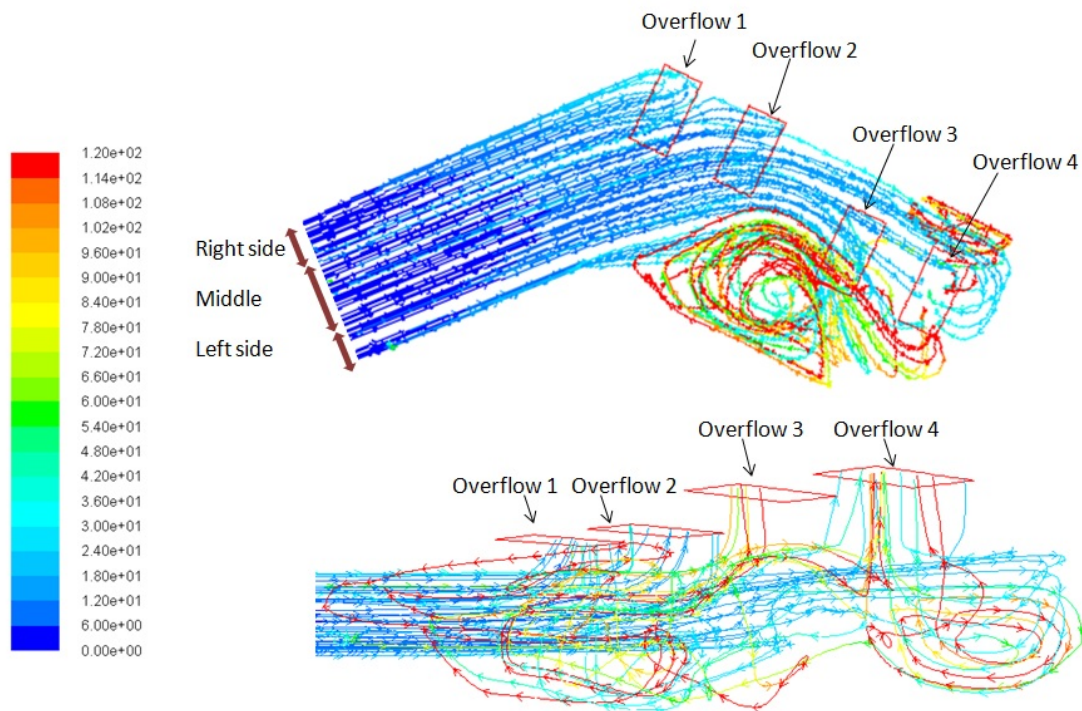
6.3.2.3 Bed Shear Stress

Figure 6.16 illustrates how inlet velocity effected the shear stress for the Århus CSO. The white areas had higher shear stress than the criteria for deposition, here set to 1Pa. Following observations where done:

- The shear stress in the inlet region was higher than the other parts of the CSO for all velocities;

- The shear stress was increasing with higher velocity;

- The overflowing CSO with velocity 0.3m/s had shear stress below 0.5Pa;

- The lowest shear stress was identified at the lower level of the CSO;

- Local areas with high velocities caused by rotations in the flow were found at the lower bed level;

- Shear stress distribution with inlet velocity 0.5m/s had high local shear stress in the left corner; and,

- The case with inlet velocity 0.7m/s had high shear stress in the inner corner after the step.
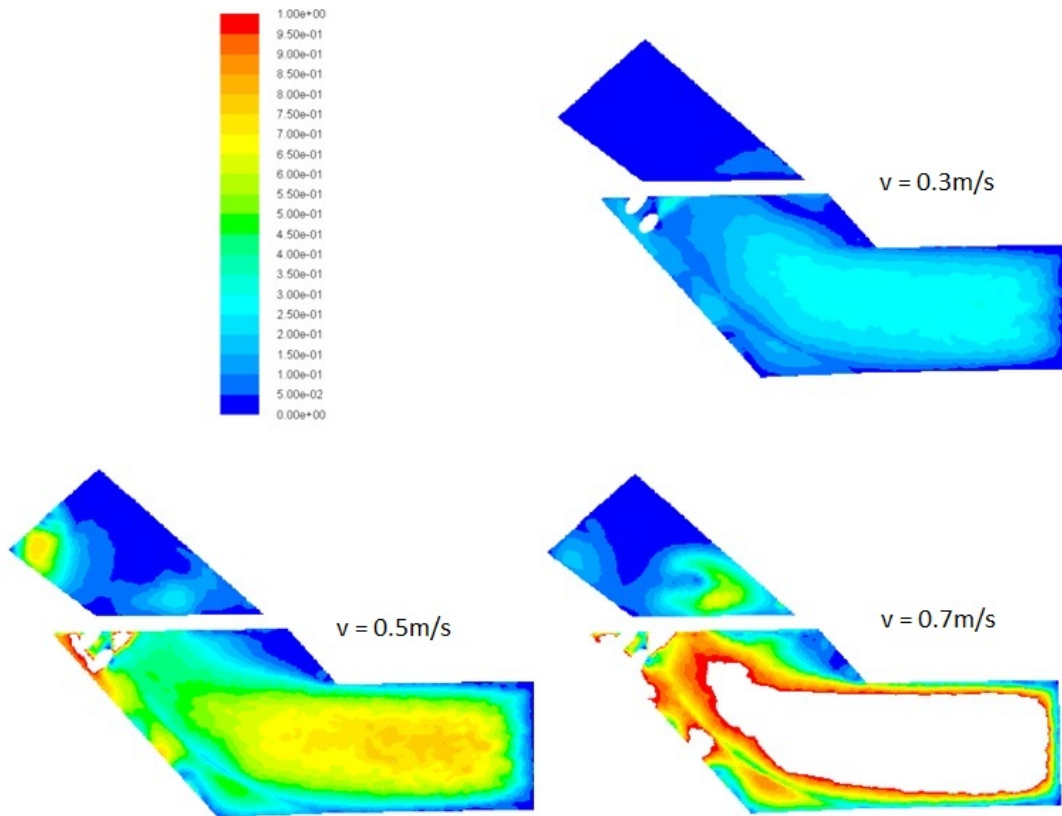
Figure 6.16: Bed shear stress for different flow conditions.

6.3.3 Discussion of Flow Scenarios

Figure 6.17 shows a comparison of the velocity magnitude. The inlet section has a similar trend for the two scenarios. The decreased maximum velocity indicates that the profile defined by the user had too large velocities in the middle. The length used to adapt the flow is, however, shorter than if a uniform inlet conditions was applied. In forthcoming work by SINTEF in conjunction with PREPARED the goal is to investigate the optimal location for water quality sensors. Accurate predictions of the velocity magnitude and direction are then needed. Inlet conditions would affect the results and the importance of applying a realistic profile must thus be emphasized.
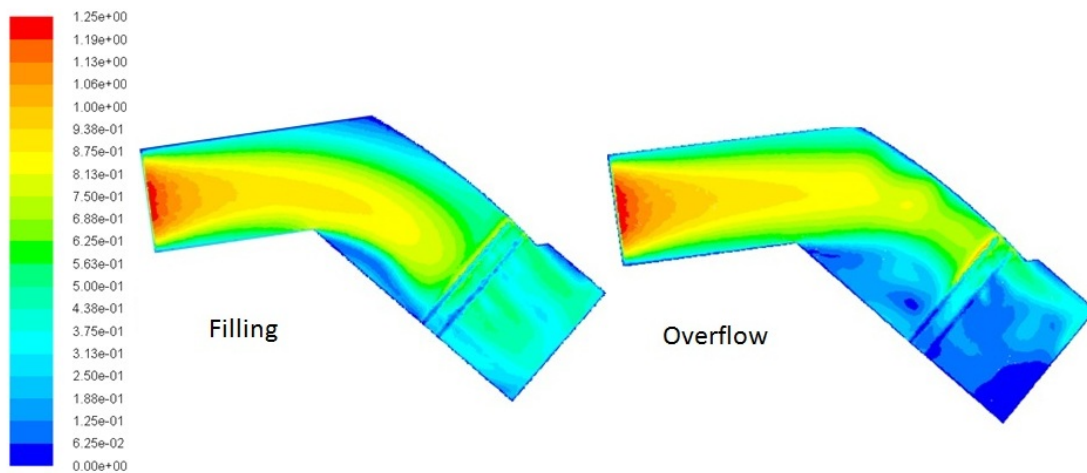
Figure 6.17: Comparison of contour plot filled and overflowing CSO.

During filling the intention is to send as much sediments to the treatment plant as possible to avoid accumulation of sediments in the CSO. High velocities are therefore desirable. Overall the flow in the CSO during filling has evenly distributed velocities, figure 6.17, and this is fortunate as it would assure self-cleansing. Blue areas have low velocities and are potential areas for sedimentation. After the corner in the inner side of CSO there is a tranquil area. It is a small area so not much sediments are expected to deposit here. The slow velocities in the outer curve seem more problematic as it is under overflow 1. If particles are deposited here they can be flushed out during overflow. To avoid this the CSO is designed with a deeper channel at the bottom, figure 6.18. It should increase the velocities at the bottom during dry-weather flow as the problem in this region is probably not so significant as first indicated.

Channel

Figure 6.18: Channel to avoid sedimentation in basin.

When the CSO is overflowing the overall goal is to prevent particles from being discharged to receiving waters. This means that deposition and accumulation of sediments are desirable during this situation. Figure 6.17 shows that there is a tranquil area after the step which enables sediments to concentrate.

The results from the flow field are the foundation to understand sediment processes. Just from analyzes of the flow field one can get information on how suspended particles moves from flow streamlines and bed shear stress can give an indication on areas where particles would accumulate. Figure 6.19 shows the contour plots of bed shear stress for the two scenarios studied. In areas that are colour sedimentation could occur, and the blue areas are most vulnerable. During filling of the CSO the shear stress after the step is high. This is caused by the strong rotations explained for the streamlines in section 6.3.1.2.
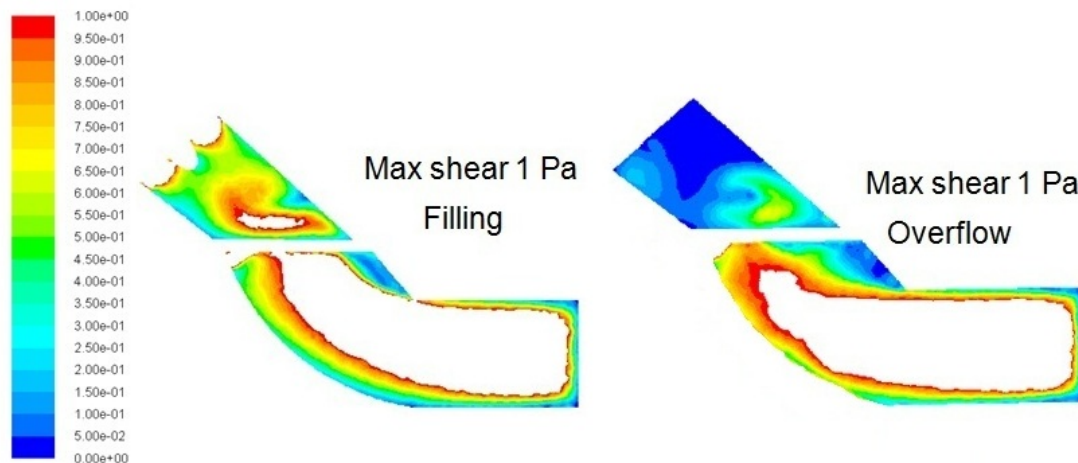
Figure 6.19: Regions with bed shear stress for filling and overflow for v=0.7m/s.

The contour plots of the BSS support the previous findings that the CSO seem to perform well both during filling and overflow. Stovin and Saul (1996) used the shear stress distribution to calculate separation efficiency as the portion of the chamber that fell below a critical shear stress value. A disadvantage of only studying the shear stress is that the characteristics of particles are not taken into account. Indirectly it is included in the threshold value for bed shear stress as it should reflect the type of sediments used. It is, however, not possible to get separation efficiency for different particle types, and the particle tracking routine will be used for this. Contour plots of bed shear stress it therefore only recommended to study possible settling locations for particles.

6.4 Particle Tracking Results

For the filled scenario it is only of interest to study the possibility of getting deposition of sediments. The separation efficiency is presented as a function of velocity for different particle types. The effect of the bed boundary condition on the results where also investigated.

6.4.1 Scenario 1 - Filling of CSO

6.4.1.1 Final Destination of Particles

Particles can either be trapped at the bottom of the CSO chamber or continue to the WWTP. Final destinations of particles are presented for particles with density 1400 kg/m^3, figure 6.20. For the trap condition particles where injected a short distance over the bottom to avoid settling at the inlet. For the BSS bound-

ary condition particles were injected over the entire inlet. The results from the two methods showed the same trends:

- Particles with diameter 0.1mm where suspended throughout the chamber and only a few particles deposited in the inner region after the bend; and,

- Particles with diameter 0.5mm showed where settled on the outer side of the curve and in some regions after the drop.
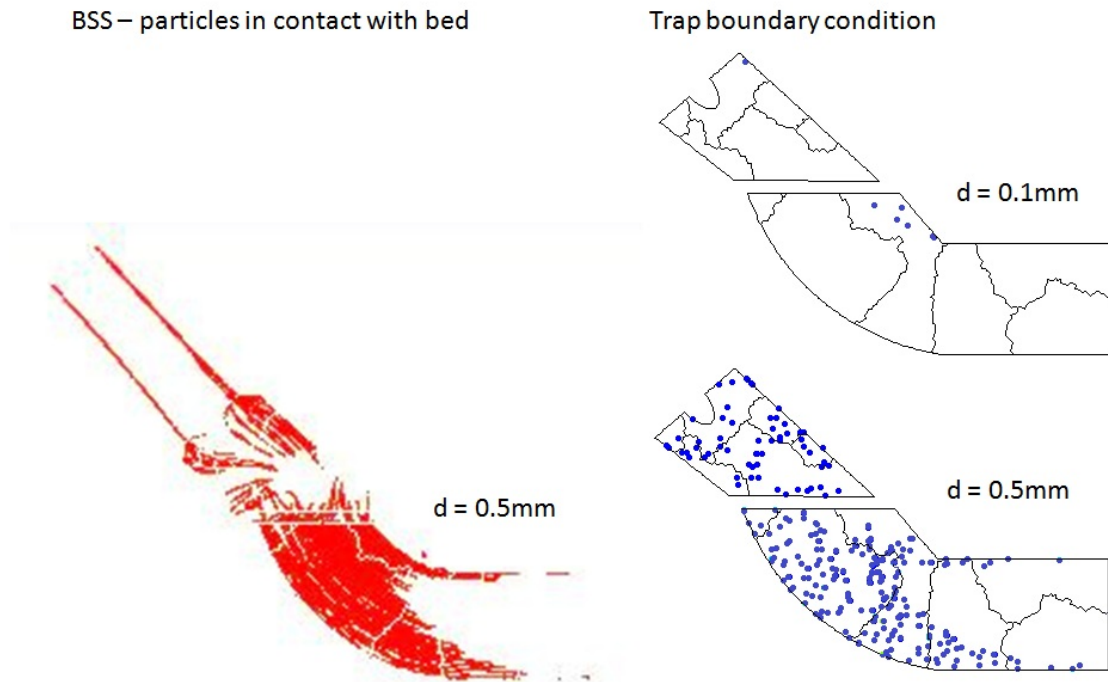
Figure 6.20: Final destination of particles on the bed during filling.

It was investigated how sediments where separated in two outlets. The reflect boundary condition was used as it was assumed that the CSO had a self-cleansing effect. 750 particles where injected and the final destination reported. The results showed that the largest amounts of sediments where sent through the right outlet, figure 6.21. The sediment fraction that escaped through the right outlet was larger for heavier particles.
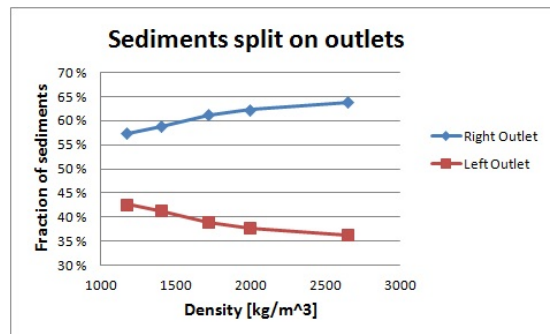
Figure 6.21: Particle fractions divided on outlets for the filled CSO.

6.4.2 Scenario 2 - Overflow of CSO

6.4.2.1 Particle Trajectories

Particle trajectories shows how sediments move in the fluid. Figure 6.22 illustrates that suspended particles, d=0.1mm, followed the streamlines of the flow and had the same particle trajectories. Since the flow field was described in section 6.3.2.2 there is no need to go into further detail here.

Particle tracks suspended particles   Flow stream lines
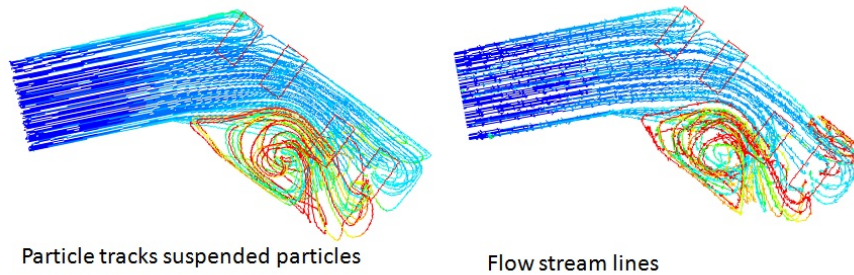
Figure 6.22: Particle tracks for suspended particles compared to flow streamlines.

Sand particles where used to show how heavy particles would behave, figure 6.23. The following observations where done:

- The particle tracks where similar for all particle sizes, but the distance before they deposited and the amount that went out of the overflows where differed;

- Due to the heavy weight of the particles they settled fast, and only a few sand particles where discharged to receiving waters;

- Almost all particles with diameter 1.0mm settled before the step;

- Some particles with diameter 0.5mm where discharged through overflow 1 and 2; and,

- It was only the 0.1mm particles that where discharged through all the overflows.

The amount of particles overflowing will be studied in more detailed with separation efficiency.
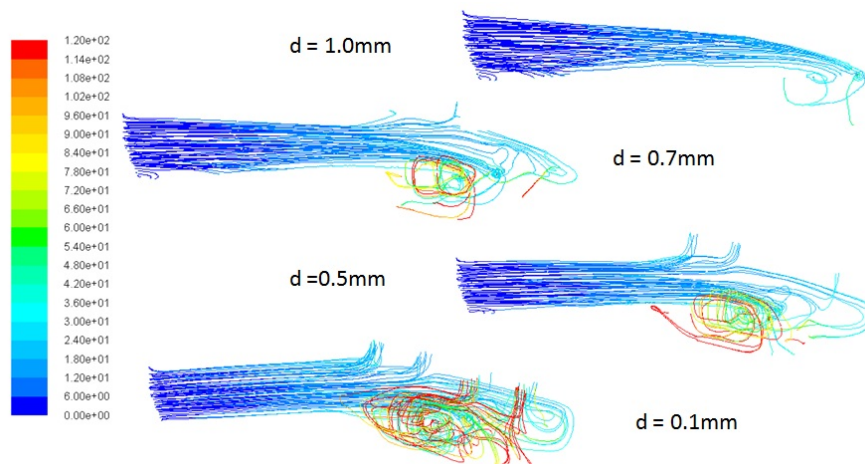
Figure 6.23: Particle tracks for sand particles during overflow.

6.4.2.2 Final Destination of Particles

Figure 6.24 shows the fraction of sediments discharged through the different overflow chambers. The density was kept constant at 1400 kg/m^3 while the particle size varied. The results showed that:

- The largest amount of particles were discharged through overflow 1 and overflow 4;

- The amount of particles discharged through overflow 3 decreased most with larger particle sizes; and,

- Overflowing of small particles where less effected by density than larger particles.
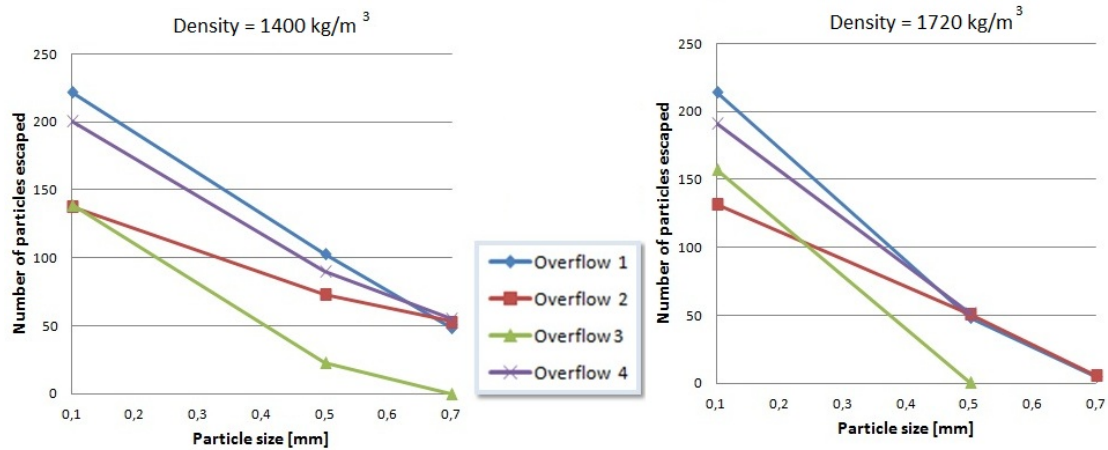
Figure 6.24: Particle fractions divided on overflows.

Residence time is the time a particle travels in the fluid until it reaches its final destination. Particles with density 1720 kg/m^3 where used to illustrate the residence time to the overflows, table 6.1. Following information was obtained from the residence time results:

- The residence time to overflow 1 and 2 was less than 30s;

- The average residence time to overflow 3 was longer than to overflow 4;

- The residence time to overflow 3 for the smallest particles was more than 2 minutes;

- The residence time to overflow 1 and 2 was increasing with particle size; and,

- The residence time to overflow 3 and 4 was decreasing with larger particles.

Particle size [mm]	Residence time [s]			
	Overflow 1	Overflow 2	Overflow 3	Overflow 4
0.1	10	4	141	74
0.5	19	18	55	31
0.7	23	21	-	-

Table 6.1: Residence time for particles escaping through overflows.

6.4.2.3 Boundary Conditions Effect on Separation Efficiency

This is a study of the sensitivity of boundary conditions on different particle types as a function of velocity. Medium sized organic material was sensitive to the boundary condition as shown in figure 6.25. The following observations where done:

- Separation efficiency at low flow velocities, here represented by velocity 0.3m/s, where less sensitive to boundary conditions compared to higher velocities;

- The trap boundary condition gave an approximately linear reduction in separation efficiency with change in velocity, also seen in appendix 4. It overestimated the efficiency for suspended particles;

- The BSS boundary condition was between the limits of trap and reflect boundaries. Separation efficiency for heavy particles where closest to the trap condition, while reflect was the best boundary condition for light and small particles the reflect boundary was the best approximation; and,

- The reflect boundary condition gave lower efficiency for the scenario with inlet velocity 0.5m/s than 0.7m/s.
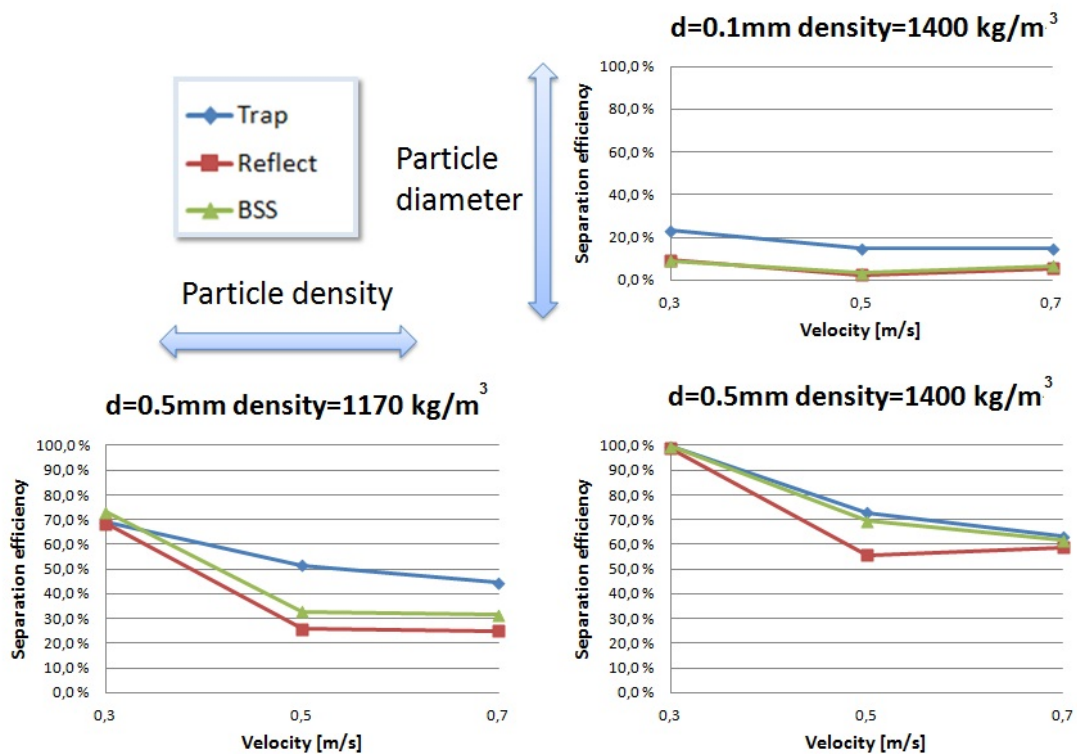
Figure 6.25: Particles where separation efficiency is affected by boundary conditions.

Density of $1400 kg/m^3$ was kept constant and diameter 0.1mm and 1mm were tested for different boundary conditions. Similarly particles with diameter 0.5mm where used to test density $1002 kg/m^3$ and $1720 kg/m^3$. Particles that would sink, high density and large size, or particles that would be suspended, low density and small size, were not affected by the boundary condition according to figure 6.26. The exception was the trap condition which overestimated the separation efficiency for small particles.
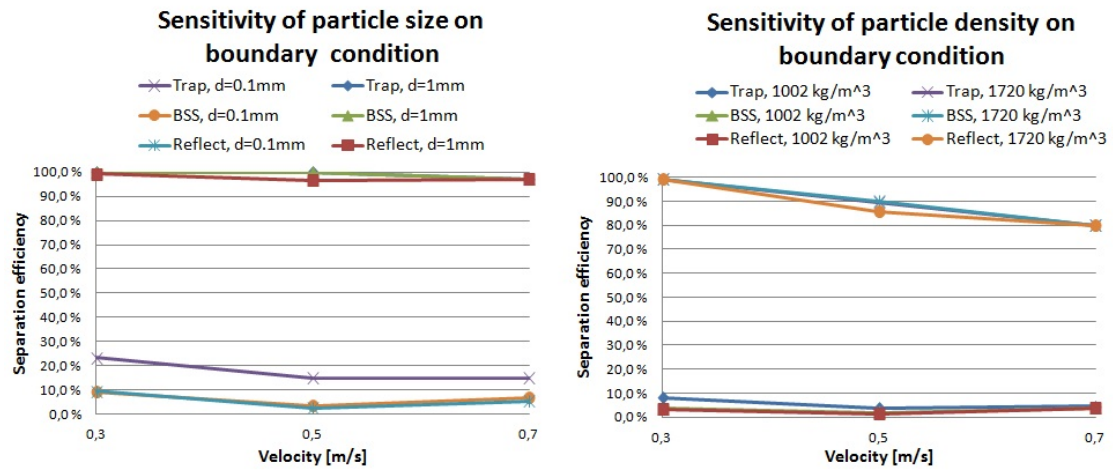
Figure 6.26: Sensitivity of particle size and density on boundary condition.

6.4.2.4 Separation Efficiency for Different Particle Types with the BSS Boundary Condition

The previous section demonstrated that the BSS boundary condition captured the physics best, and was applied for the analyzes of separation efficiency. The influence particle size had on the separation efficiency was investigated, figure6.27, and the effect of density, figure 6.28. Comments on the separation efficiency are presented in the following:

- Separation efficiency of settable solids was dependent on inlet velocity;

- Separation efficiency decreased most when the flow was increased from 0.3m/s to 0.5m/s;

- The particles most influenced by a change in velocity from 0.3m/s to 0.5m/s (d=0.5mm and $\rho = 1170kg/m^3$) lost 40% of the efficiency;

- The reduction in separation efficiency with change in velocity was larger for particles with $\rho = 1170kg/m^3$ than $\rho = 1400kg/m^3$ for all particle sizes;

- Particles with diameter 0.1mm had less than 10% separation efficiency for velocities 0.5m/s and higher independent of density;

- Sand particles, $\rho = 2650kg/m^3$, only discharged particles less than 0.5mm;

- The separation efficiency for 0.1mm sand particles was approximately 50%;

- Particles with $\rho = 2000kg/m^3$, had separation efficiency with more than 90% for all velocities;

- The reduction in separation efficiency was almost halved when reduced from 1400 kg/m^3 to 1170 kg/m^3; and,

- Floating particles, $\rho = 1002kg/m^3$, had 20% or less separation efficiency when the velocity was 0.5m/s and higher for particles up to 5mm.
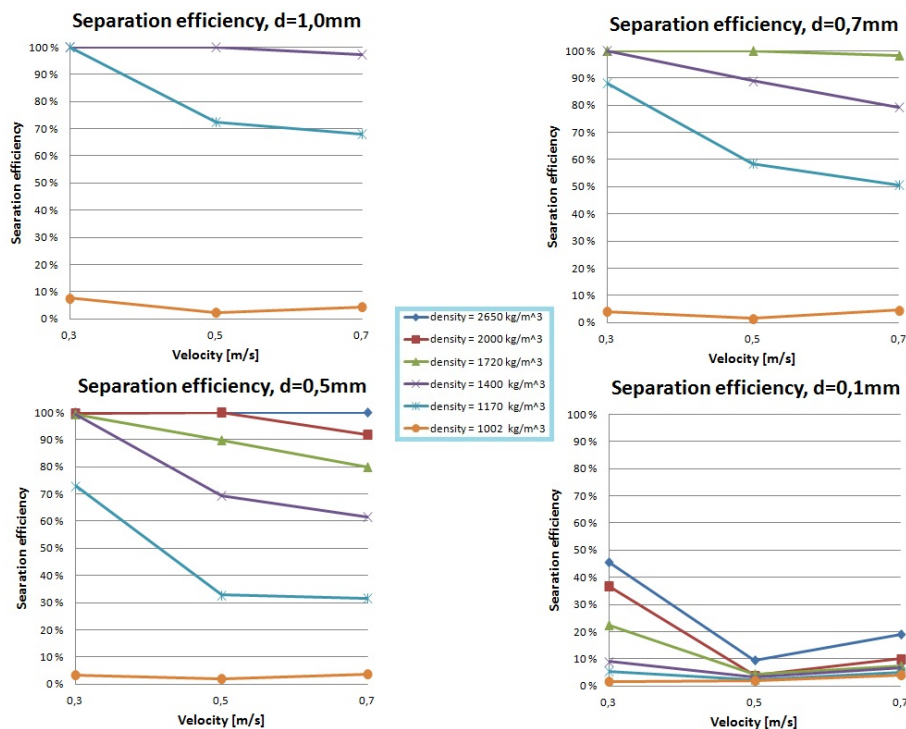
Figure 6.27: Separation efficiency dependent on particle size.
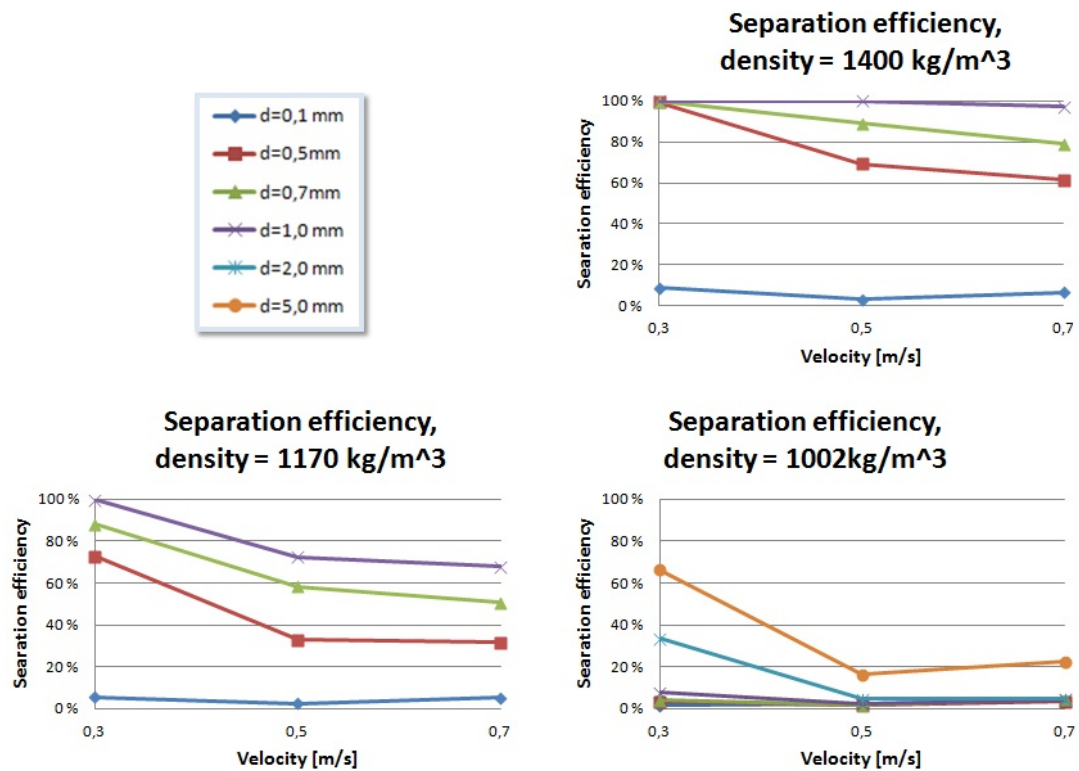
Figure 6.28: Separation efficiency dependent on density.

6.4.3 Discussion of Particle Tracking Results

For the filling scenario it was only of interest to determine particles final destination to identify potential areas for settling of sediments. As shown in the results, figure 6.20, it is possible to plot the point of impact on the bed both with the trap and BSS boundary condition. It is, however, a demanding operation as it is not an integrated post-processing option in FLUENT. The results were in agreement with the bed shear stress plots, figure 6.19, and the author therefore recommend to rather plot shear stress as an indicator of where settling of sediments can occur.

Particle tracks coloured by residence time and summary reports of final destination were more useful. The results showed that recirculation zones had a strong influence on the particles. The fraction of particles divided on outlets for the filled CSO, figure 6.21, showed that the light weighted particles were dragged into the recirculation zone and thus escaped through the left outlet. Heavier particles were not as much affected by the turbulent region and a larger fraction escaped through the right outlet. Also in the overflow structure, it was seen that the amount of particles that escaped through overflow 3 decreased with particle size. This can be explained based on the flow streamlines which showed that the flow from the recirculation zone after the step discharged through overflow 3. The summary report also gives the residence time of each boundary and shows the time particles use to reach the final destination. The results showed that the residence time to overflow 1 and 2 was relatively short. This was expected as the streamlines went directly into the overflows. The residence time to overflow 3 and 4 was significantly longer especially for suspended particles that where entrained in flow rotations.

The literature review prior to the modelling emphasized the importance of defining appropriate boundary conditions. The results showed that medium sized organic sediments where effected by the bed boundary conditions. The largest difference in separation efficiency between the trap and reflect boundary condition was 20% (d=0.5mm & $\rho = 1170 kg/m^3$). The trap boundary condition over predicted the efficiency, especially for small particles. This was expected as the particles would stick at the first contact with

the boundary independent of the velocity of the fluid or size of the particle. The error due to the trap boundary condition was also expected to increase with larger velocity. This was also seen in the results for d=0.5mm and $\rho = 1170 kg/m^3$. For smaller particles that were suspended at all times, the difference between the boundary conditions were almost constant independent of velocity.

The reflect boundary condition was expected to under predict separation efficiency, and this was confirmed by the results. It was not predicted, however, that the separation efficiency for the case with velocity 0.5m/s would be lower than for 0.7m/s. This is illustrated for more scenarios in appendix 5. Normally one would expect a decrease in separation efficiency with higher velocity. This is also the result from the BSS boundary condition. The reflect boundary condition therefore underestimates the separation efficiency, and especially for the case with velocity 0.5m/s where the flow pattern is unfavourable.

If any of the default boundary conditions are to be used, the reflect boundary condition is recommended as it gives a conservative approach. The BSS boundary condition is, however, the recommended approach as it captured the physics best and seemed to give reasonable results. As the literature review showed sensitivity to the threshold value used for this boundary conditions, measurements of the bed shear stress would be preferably. In the following analyzes of separation efficiency this is the boundary condition applied.

The separation efficiency results were not validated as no sediment samples were available from Århus at the time when this study was conducted. But previous CFD modelling compared to laboratory experiments have shown that the particle tracking routine probably over predicts the separation efficiency for high velocities, figure 6.29 (Stovin & Saul, 1998). This is because it is only the settling process that is modelled, and not the erosion process. With an increase in velocity the previous settled sediments are likely to be re suspended as it is a dynamic process.
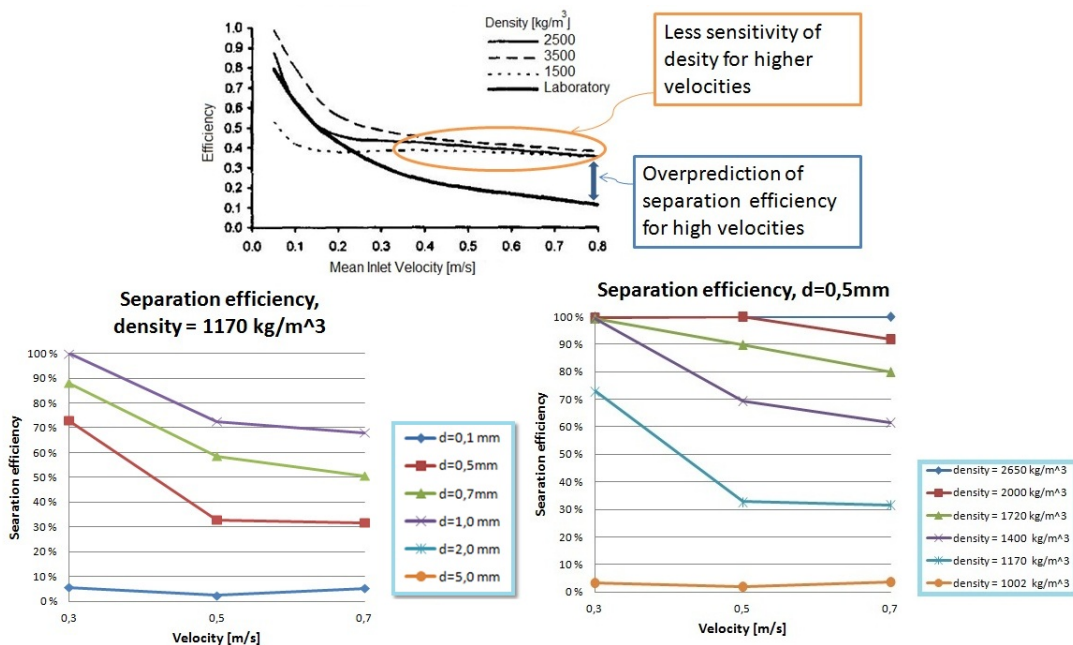
Figure 6.29: Comparison with previous studies.

Stovin and Saul also found that separation efficiency was less sensitive to a change in density for higher velocities. This was not observed in the results from this study. The reason for this may be that the velocities tested were not high enough to capture this trend. The conclusions from the results is that both density and particle size have a strong influence on the separation efficiency. The effect of the particle properties have less influence when the velocity increases. The results also showed that the higher amount of organic material the lower separation efficiency.

53

Chapter 7

Conclusion

This report has demonstrated how numerical modelling can be used to give better understanding of sediments behaviour in a CSO. The main conclusions are listed in the following:

- The flow field during overflow and filling have different characteristics as seen from contour plots and flow streamlines;

- There is a strong correlation between the streamlines of the flow field and particle tracks for suspended particles;

- It is evident that recirculation zones have an influence on sediment transport and particles final destination. Light weighted and small particles are most affected;

- Shear stress distribution at the bed should be used to predict particle deposition locations during filling of a CSO;

- It is crucial to define appropriate boundary conditions as it has a significant effect on the result. In this work a fully developed velocity profile was defined at the inlet and a shear stress criteria at the bed;

- The bed shear stress (BSS) boundary condition was applied successfully. The critical value for deposition was found to be 1.0 Pa for a typical combined sewers with sand traps;

- The particle tracking routine over predicts the separation efficiency for high velocities as erosion is not included in the boundary conditions;

- Density and particle size has a strong influence on the separation efficiency;

- The particle properties have less influence on the separation efficiency with increasing velocity;

- The strictest criterion for separation efficiency from the Austrian Guidelines ÖWAV-RB (2007) is 40%. According to this standard the Århus geometry has a good quality function; and,

- The particles that would overflow are small particles with diameter 0.1mm, floating particles with density $1002 kg/m^3$ and particles with diameter 0.5mm and density $1170 kg/m^3$.

Chapter 8

Further Work

In the last phase of the project some new discoveries where found in the CSO. Additional two outlets where identified after the inlet and at the back edge, figure 8.1 (Skjetne, 2012). The two new overflows account for a significant percentage of discharge to the receiving waters. The new discoveries will thus have an effect on the flow field in the geometry and will influence the separation efficiency. As the master thesis was ending, there was no time to investigate this. The modelling of the CSO geometry presented in chapter 6 is still valid. This is because the results must be seen in the context of set-up and premises that the model is built on, and be interpreted according to the geometry in figure 6.1. The methods for investigations are the same and have been demonstrated in this report. Some knowledge is however gained from this incident: At the early stages of the project a cite visit should be done by the people that should interpret the technical drawings. This is important to avoid misinterpretations, and will save time and costs.
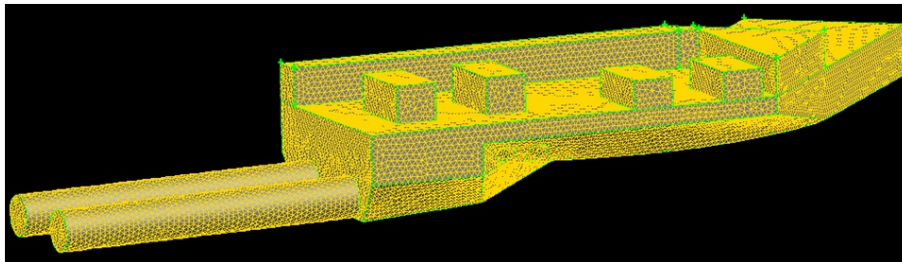

Figure 8.1: Modified geometry (Skjetne, 2012).

Manual sampling of the sediments that goes in and out of the CSO should also be done. This is important for validation purposes of the numerical model. Measurements are also important to study the development over time and discover changes due to climate change.

Bibliography

Aaby,   L. (2011). Overløp - En kritisk komponent i avløpssystemet. pp. 80

Adamsson, Å., Stovin, V. & Berghdal, L. (2003). Bed Shear Stress Boundary Condition for Storage Tank Sedimentation. *J. Environmental Engineering*, pp. 651-658

Adamsson, Å., Berghdal, L. & Lyngfelt, S. (2005). Measurement and Three-dimensional Simulation of Flow in a Rectangular Detention Tank, *Urban Water J.*, vol. 2, no. 4, pp. 277-287

ANSYS   Inc. (2010a). ANSYS FLUENT User's Guide, pp. 2266

ANSYS   Inc. (2010b). ANSYS FLUENT Theory Guide, pp. 703

ANSYS   Inc. (2011a). FLUENT- Realize Your Product Promise. Retrieved May 14, 2012 from http://www.ansys.com/staticassets/ANSYS/staticassets/resourcelibrary/brochure/ansys-fluent-brochure-14.0.pdf

ANSYS   Inc. (2011b). Introduction to ANSYS FLUENT - Turbulence. Sheffield. pp. 46

Ashley,   R.M., Wotherspoon, D.J.J., Coghlan, B.P. & McGregor, I. (1992). The Erosion and Movement of Sediments and Associated Pollutants in Combined Sewers, *Wat. Sci. and Tech.*, vol. 25, no. 8, pp. 101-114

Ashley,   R.M., Crabtree, R.W. (1992) Sediment origins, deposition and build-up in combined sewer systems *Wat. Sci. and Tech.*, vol. 25, no. 8, pp. 1-12

Ashley,   R.M., Longair, I.M., Wotherspoon, D.J.J. & Kirby, K. (1993). Flow and Sediment Movement Monitoring in Large Sewers, *Wat. Sci. and Tech.*, vol. 28, no. 11-12, pp. 55-65

Bares,   V., Jirak, J. & Pollert, J. (2006). Bottom Shear Stress in Unsteady Sewer Flow, *Wat. Sci. and Tech.*, vol. 54, no. 6-7, pp. 93-100

Berg,   A. (1988) Sjølvrensing og spyling av avløpsledninger. Trondheim: Norges Teknisk-Naturvitenskapelige Forskningsråd. pp. 91

Bruaset,   S., Hem, L.J., Ugarelli, R. (2011) *Water Quality Sensors Micro − location in Sewers* pp. 46-54

Dufresne,   M., Vazquez, J., Terfous, A. Ghenaim, A. & Poulet, J.-B. (2009). Experimental Investigation and CFD Modelling of Flow, Sedimentation and Solid Separation in a Combined Sewer Detention Tank. *Computers and Fluids* vol. 38 pp. 1042-1049

Butler,   D. & Davis, J.W. (2011) Urban Drainage. London: Spon Press. pp. 625

European Communities (2000) Directive 2000/60/EC of the European Parliament and of the Council of 23 October 2000 establishing a framework for Community action in the field of water policy. The European Parliament and of the Council of the European Union. pp. 72

Faram,   M.G. & Harwood, R. (2003). A Method for the Numerical Assessment of Sedeiment Interceptors, *Wat. Sci. and Tech.*, vol. 47, no. 4, pp. 167-174

Field,   R. & O'Connor (1996). SWIRL Technology: Enhancement of Design, Evaluation, and Application. *Journal of Environmental Engineering, ASCE*, pp. 35.

Harwood,   R. (1998). Modelling of Combined Sewer Overflow Chambers Using Computational Fluid Dynamics. PhD Thesis, University of Sheffield.

Huntington Sanitary Board (2004). How a Combined Sewer System Works. Retrieved April 29, 2012 from http://www.huntingtonsb.com/images/combined-sewer-overflow.jpg

Khan,   L.A., Wicklein, E.A., Rashid, M. (2005). A 3D CFD Model Analysis of Hydraulics of an Outfall Structure at a Power Plant, *J. Hydro− informatics*, vol. 7, no. 4, pp. 283-290

Kleidorfer, M. & Rauch, W. (2011). An Application of Austrian Legal Requirements for CSO Emissions, *Wat. Sci. and Tech.*, vol. 64, no. 5, pp. 1081-1088

Luyckx,   G., Vaes, G. & Berlamont, J. (1999). Experimental Investigation on the Efficiency of a High Side Weir Overflow, *Wat. Sci. and Tech*, vol. 39, no. 2, pp. 61-68

Luyckx,   G., Vaes, G. & Berlamont, J. (2005). Solids Separation Efficiency of Combined Sewer Overflows, *Wat. Sci. and Tech*, vol. 51, no. 2, pp. 71-78

Malvern   Instruments Ltd (2012). Laser Diffraction. Retrieved 20 May 2012, from

www.malvern.com/labeng/technology/laser_diffraction/laser_diffraction.htm

Michelbach, S. & Wöhrle, C. (1992). Settlable Solids in a Combined Sewer System - Measurement, Quantity, Characteristics, *Wat. Sci. and Tech*, vol. 25, no. 8, pp. 181-188

Nazaroff, W.W. & Alvarez-Cohen, L. (2001). Environmental Engineering Science. Berkeley: Jhon Wiley & Sons, Inc. pp. 690

Paus,   K. (2011, September 8). Overvannskvalitet. *Presentation Presented*

in TV M6002 at NTNU, Trondheim, pp. 1-36

Pipelife   Norge AS (2007). Rørhåndboka, pp. 75

Pollert,   J. & Stransky (2002). Combination of Computational Techniques - Evaluation of CSO Efficiency for Suspended Solids Separation, *American Society of Civil Engineers*, pp. 10

PREPARED Report no. 2011.031 (2011). Definition of Methods for Optimal Micro-Location of Sensors in Sewers. pp. 66

PREPARED Enabling Change (2012). Retrieved 20 March 2012, from www.prepared-fp7.eu.

Raudkivi, A.J. (1998). Loose Boundary Hydraulics, 4th. edn. A.A. Balkema, pp. 512

Saul   A.J. & Svejkovsky, K. (1994). Computational Modeling of a Vortex CSO Structure, *Wat. Sci. and Tech.*, vol 30, no 1, pp. 9

Schmitt,   F., Milisic, V. , Bertrand-Krajewski, J.-L., Laplace, D. & Chebbo, G. (1999). Numerical Modeling of Bed Load Sediment Traps in Sewer Systems by Density Currents, *Wat. Sci. and Tech*, vol. 39, no. 9, pp. 153-160

Skjetne,   P. (2012). CFD Modelling of CSO, *IWA Congress on Water Climate and Energy*, Dublin. pp. 26.

Slater,   J. (2008, July 17). NPARC Alliance CFD Verification and Validation. Retrieved December 2, 2011 from NASA: www.grc.nasa.gov/www/wind/valid/resources.html

Stovin,   V.R. & Saul, A.J. (1996). Efficiency Prediction for Storage Chambers using Computational Fluid Dynamics. *Wat. Sci. and Tech.*, vol. 33, no. 9, pp. 163-176

Stovin,   V.R. & Saul, A.J. (1998). A Computational Fluid Dynamics (CFD) Particle Tracking Approach to Efficiency Prediction, *Wat. Sci. and Tech.*, vol. 37, no. 1, pp. 285-293

Toffol,   S. De (2006). Sewer System Performance Assessment - An Indicators based Methodology (Doctoral dissertation). Retrieved from University of Innsbruck, Germany.

Ugarelli,   R. (2011). Transition Flow . Bologna University.

Vazquez,   J., Zug, M., Buyer, M. & Lipeme, G. (2005). CSOs: Tools for Assessing their Operation in Our Systems, *Wat. Sci. and Tech.*, vol. 51, no. 2, pp. 179-185

Vosswinkel N. (2010), Numerische Strömungssimulation zur Unterstützung von Messkampagnen mittels Kreuzkorrelation unter besonderer Berücksichtigung des Sensornahbereiches, MSc, *Muenster University of App* pp. 201.

White,   F.M. (2006). *Viscous Fluid Flow*.Kingston: McGraw-Hill Higher Education, pp. 629.

Wickenheiser, M. (2012, May 4). Maine Not Alone in Expensive Sewer-Stormwater Overflow Problems. Retrieved May 09, 2012 from http://www.chicagotribune.com/news/sns-mct-maine-not-alone-in-expensive-sewer-stormwater-20120504,0,2423533.story

Appendix 1: UDF for Bed Shear Stress

```c
#include "udf.h"
#define critical_shear 1.0

DEFINE_DPM_BC(bc_shear,p,t,f,f_normal,dim)
{
    /*Computing shear stress*/

    real area;
    real wShear;
    real A[ND_ND];
    int zone_id = THREAD_ID(t); /*satte inn = THREAD_ID(t)*/

    F_AREA(A,f,t);
    wShear = NV_MAG(F_STORAGE_R_N3V(f,t, SV_WALL_SHEAR)) / NV_MAG(A);



    if(wShear > critical_shear)
    {
        return PATH_ACTIVE;
    }
    else {
        zone_id = Lookup_Thread(domain,zone_id);
        trap_count[zone_id] += 1;
        return PATH_ABORT;
    }
}
```

Appendix 2: Legislation for CSO Emissions

Overview on the requirements for CSOs in European member states and USA elaborated from (Fenz, 2002; Gamerith, 2006; Krejci, 2004; UNEP, 2002; Zabel et al., 2001). % CSS is the percentage of combined sewer system in each country; treatment rate is the percentage of wastewater that should be treated at the treatment plant.

Country	Guideline	% CSS	Q_{wwtp}	Q_t (CSO)	Required storage volume	Treatment Rate considered	Effects on RW considered
Austria	(ÖWAV-Regelblatt 19, 1987)	75-80	$2\,Q_{DWFp}$	<15 $l/(s\cdot ha_{Ared})$	15-25 m^3/ha_{Aimp}	no	no
Austria new	(ÖWAV-Regelblatt 19, Draft 11.2005)		$2\,Q_{DWFp}$			50% rain runoff (tab 2-2)	yes
Belgium (Flanders)		70	$3\text{-}5\,Q_{DWFm}$	5-10 Q_{DWFm} NO=7/a	Remaining spilling vol. with T = 1/7 year	no	yes
Denmark		45-50	$2\,Q_{DWFp}$	5 Q_{DWFp} NO=2-10/a		no	yes
Finland		10-15	$2\,Q_{DWFp}$	6-7 Q_{DWFm}		no	
France	(CERTU, 2003)	70-80	$2\text{-}3\,Q_{DWFm}$	3 Q_{DWFp}	Interception of rainfall with T = 3-6 months	no	sometime
Germany	(ATV - A 128, 1992; BWK, 2001)	67	$2\,Q_{DWFp}$	7.5-15 $l/(s\cdot ha_{Aimp})$	10-40 m^3/ha_{Aimp}	90% of COD load	yes
Greece		20	$2\,Q_{DWFm}$	3-6 Q_{DWFm}		no	sometime
Ireland		60-80	$3\,Q_{DWFm}$	6-9 Q_{DWFm}		no	sometime
Italy	Local e.g. (Regione Toscana, 2006)	60-70	$2\,Q_{DWFm}$	3-5 Q_{DWFm}		no	sometime
Luxembourg	(ATV - A 128, 1992)	80-90	$2\text{-}3\,Q_{DWFm}$	7.5-15 $l/(s\cdot ha_{Aimp})$	10-40 m^3/ha_{Aimp}	no	
Netherlands		74	$3\,Q_{DWFp}$	5 Q_{DWFm} NO = 3-10/a	ca. 70 m^3/ha Aimp	no	sometime
Portugal		40-50	$2\,Q_{DWFm}$	6 Q_{DWFm}		yes	sometime
Spain		70	$2\,Q_{DWFm}$	5 Q_{DWFm}		no	no
Sweden		25-40	$3\text{-}4\,Q_{DWFm}$	5-20 Q_{DWFm}		no	
Switzerland	(AfU, 1977; GSchG, 1991; GSchV, 1998)		$2\,Q_{DWFp}$			no	yes
UK	(FWR, 1998)	70	$3\,Q_{DWFm}$	6-9 Q_{DWFm}	t_D= 2h at 3 Q_{DWF}	no	yes
USA	(CWA, 1997; US EPA, 1995)			NO=4-6 /a		85% combined wastewater	yes

Where:

Q_{wwtp}	Wastewater flow rate to wastewater treatment plant allowed
Q_t	Throttle discharge at CSOs
Q_{DWFm}	Mean dry weather flow
Q_{DWFp}	Dry weather flow (daily peak)
T	Return period
NO	Number of overflow per year
t_D	Detention time
A_{imp}	Impervious area connected to the combined sewer system

Appendix 3: UDF for Fully Developed Velocity Profile for Square Inlet

```c
/*v=0.1 Q=0.48 */
#include "udf.h"
#include <math.h>

#define PI 3.14159265

DEFINE_PROFILE(inlet_x_velocity, thread, position)
{
int width_dir, height_dir;
real i;
real x[ND_ND];
real vel_in;
real width, height, my_viscosity;
real global_offset[3];
real dpdx, sum_tanh, Q_flow;
real width_pos, height_pos;
face_t f;


/* INITIALIZE SOME VARIABLES */
width_dir                = 1;        /* coordinate direction for width of channel X=0, Y=1, Z=2 */
height_dir               = 2;        /* coordinate direction for height of channel X=0, Y=1, Z=2 */
width                    = 3.9592;   /* width of channel at inlet [m] */
height                   = 1.205;    /* height of channel at inlet [m] */
global_offset[width_dir]  = width*0.0;  /* the offset of the global coordinate system
                                           if it is not located at the centre of the channel */

global_offset[height_dir] = height*0.0; /* the offset of the global coordinate system
                                           if it is not located at the centre of the channel */

my_viscosity             = 0.001;   /* effective viscosity of the fluid in the channel */

/* FOR A SPECIFIDE FLOW RATE, CALCULATE THE PRESSURE GRADIENT */
Q_flow                   = 0.48;    /* The total flow rate in the channel [m3] */
sum_tanh                 = 0.0;     /* temporary variable to precalculate sum used for
                                        estimating pressure gradient */


/* LOOP OVER ALL THE INLET FACES AND CALCULATE THE VELOCITY AND SET THE VELOCITY IN THE PROFILE */
begin_f_loop(f, thread)
{
    F_CENTROID(x, f, thread);
    width_pos  = x[width_dir]  - global_offset[width_dir];
    height_pos = x[height_dir] - global_offset[height_dir];
    vel_in     = 0.0;
    for(i = 1.0; i < 16.0; i+=2.0)
    {
        vel_in += pow ((-1.0), ((i-1.0)/2.0))
                * ( 1.0-(   cosh(i*PI*height_pos/width) / cosh(i*PI*0.5*height/width) ) )
                * cos(i*PI*width_pos/width)/(i*i*i);
    }
    vel_in *= (4.0*width*width)/(my_viscosity*PI*PI*PI);
    F_PROFILE(f, thread, position) = 0.0.001022335*vel_in;
}
end_f_loop(f, thread)
}
```

Calculation of Q and $\frac{dp}{dx}$:

i	prefactor	term	product
1	1	0	0
3	-1	0	0
5	1	0	0
7	-1	0	0
9	1	0	0
11	-1	0	0
13	1	0	0
15	-1	0	0
SUM			0
Prefactor	2022,205		0

0

2a =	width	3,9592	m
2b =	height	1,205	m
y :	width_pos	0	m
z :	height_pos	0,6025	m
μ	viscosity	1,00E-03	Pa.s
l	liters	1,59E-04	m3
l/s	Q_flow	0,48	m3/s
	A_inlet	4,77	m^2
		0,100	

Want to solve for -dp/dx

i	term
1	0,444703665
3	0,003672969
5	0,000314675
7	5,93517E-05
9	1,69289E-05
11	6,20888E-06
13	2,69327E-06
15	1,31687E-06
SUM	0,448777809
Prefactor1	6232,009738
Prefactor2	2,061447406
Full term	466,5790395
-dp/dx	0,001022335

Rectangular section: $a < y < a, \quad b < z < b$:

$$u(y,z) = \frac{16a^2}{\mu\pi^3}\left(\frac{dp}{dx}\right)\sum_{i=1,3,5,\ldots}^{\infty}(-1)^{(i-1)/2}\left[1 - \frac{\cosh(i\pi z/2a)}{\cosh(i\pi b/2a)}\right]$$

$$\times \frac{\cos(i\pi y/2a)}{i^3} \qquad (3-48)$$

$$Q = \frac{4ba^3}{3\mu}\left(-\frac{dp}{dx}\right)\left[1 - \frac{192a}{\pi^5 b}\sum_{i=1,3,5,\ldots}^{\infty}\frac{\tanh(i\pi b/2a)}{i^5}\right]$$

v

Appendix 4: Separation Efficiency for Trap Boundary Condition
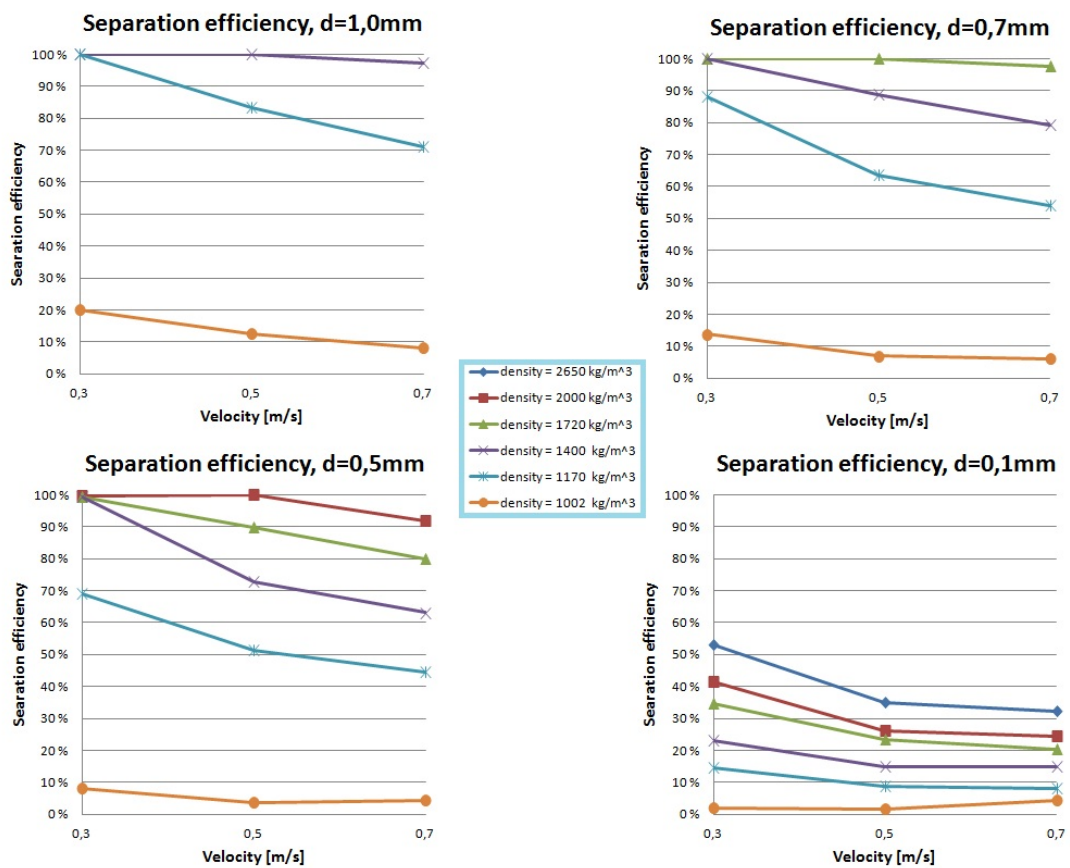
Appendix 5: Separation Efficiency for Reflect Boundary Condition